Computers and Mathematics with Applications 161 (2024) 13–31

Contents lists available at ScienceDirect

Computers and Mathematics with Applications

journal homepage: www.elsevier.com/locate/camwa

A second-order time parallel decoupled algorithm for the Stokes/Darcy model

Dandan Xue [a], Yanren Hou [b,c,*], Yi Li [d]

[a] College of Mathematics and Physics, Chengdu University of Technology, Chengdu, Sichuan 610059, China
[b] College of Mathematics and System Science, Xinjiang University, Wulumuqi 830046, China
[c] School of Mathematics and Statistics, Xi'an Jiaotong University, Xi'an, Shaanxi 710049, China
[d] School of Mathematics, Northwest University, Xi'an, Shaanxi 710127, China

ARTICLE INFO

Keywords:
Time parallelization
Decoupled method
Parareal
Spectral deferred correction
Stokes-Darcy model

ABSTRACT

This paper focuses on investigating a second-order time parallel decoupled algorithm for the mixed Stokes/Darcy model. The main objective of this algorithm is to deal with the issue of low computational efficiency in solving the coupling problem directly. Our scheme not only reduces the computation scale through the decoupling method, but also realizes the parallelism in the time direction through parareal method. Furthermore, we implement a second-order spectral deferred correction method to improve accuracy. For some small time step size, we prove the stability and convergence results of the time parallel decoupled algorithm. Finally, we provide three numerical tests to demonstrate the reliability and computational efficiency of our algorithm.

1. Introduction

The mixed Stokes/Darcy model is one of the most widely used models for the coupled between the incompressible flow and the porous media flow [1–8]. The coupling model is capable of simulating the interaction between the motion of fluids on the surface and subsurface. Specifically, it combines the Stokes equations to describe the fluid flow in the surface region, and the Darcy equations to govern the porous media flow in the subsurface region. In addition, the model couples these two flows through certain interface conditions.

Up to now, there is a rich literature on the numerical methods for the mixed Stokes/Darcy model [9–20]. These numerical schemes can be divided into two types: one solves it directly, the other is to decouple this coupling model. In the early studies, scholars mainly studied the numerical methods to directly solve the coupling problem. But the mixture of coupled models will lead to various mathematical and numerical difficulties [10], such as the large calculation scale, limited computing resources, programming difficulties and so on. However, the decoupling algorithms can significantly reduce the computational scope of the original coupled problem. Since the decoupled sub-problems are relatively simple and independent of each other, one can solve them individually or in parallel using different numerical methods and the existing packages. Therefore, many scholars devote themselves to the study of efficient and stable decoupling algorithms for solving the coupled systems. For the unsteady Stokes/Darcy model, Mu and Zhu [21] first studied a decoupled scheme, which is based on interface approximation via temporal extrapolations. As an extension of the decoupling approach, the multiple-time-step techniques were analyzed in [22–27], allowing the different time steps in different regions to improve the computational efficiency. In [28], Qin et al. proposed an adaptive time-stepping decoupled algorithm for the coupled Stokes/Darcy model, which combines the variable time-stepping decoupled algorithm with the adaptive algorithm together to decrease the calculation steps and truncation errors. Thus, it can be further improved the computation efficiency.

With the rapid development of super-parallel computers, how to design efficient parallel numerical algorithms has become a hot topic in the field of computational mathematics. Various spatial parallel algorithms have been proposed [29–31], which can greatly improve the computational efficiency. However, there is a limitation, that is, with the increase of the number of processors, the parallel efficiency of the algorithm will reach saturation which will lead to the waste of computing resources. Therefore, more and more attention has been paid to the time parallel algorithms.

The parareal method, initiated by Lions, Maday and Turinici in [32], implements the parallelization of ordinary differential equations or the discretized partial differential equations by time decomposition. The parareal method calculates the solution of the differential equations iteratively

* Corresponding author at: College of Mathematics and System Science, Xinjiang University, Wulumuqi 830046, China.
E-mail addresses: xuedandan@cdut.edu.cn (D. Xue), yrhou@mail.xjtu.edu.cn (Y. Hou), liyizz@nwu.edu.cn (Y. Li).

https://doi.org/10.1016/j.camwa.2024.02.033
Received 23 August 2023; Received in revised form 9 January 2024; Accepted 16 February 2024

by assigning a processor to each time subinterval throughout the entire time domain. Normally, the parareal method involves two numerical approximation methods, represented as $\mathscr{G}$ and $\mathscr{F}$. The parareal method proceeds by iteratively alternating between the parallel computation of $\mathscr{F}$ and the sequential calculation of $\mathscr{G}$. The details of the stability and the convergence of parareal method can be found in [33,34]. For the sake of efficiency of parareal method [33,35], the numerical cost of the $\mathscr{G}$ propagator needs to be comparatively lower than that of the $\mathscr{F}$ propagator. Let us consider the initial value problem

$$\begin{cases} y'(t) = F(t, y(t)), \quad t \in [0, T], \\ y(0) = y^0, \end{cases}$$

with $y(t)$, $y^0 \in \mathbb{C}^d$ and $F : \mathbb{R} \times \mathbb{C}^d \to \mathbb{C}^d$. Following the general strategy of parareal method, the time interval $[0, T]$ can be divided into N intervals with each subinterval being assigned to a different processor. If we denote the processors P_1 through P_N, the n-th processor computes the solution on the subinterval $[t^n, t^{n+1}]$, $n = 0, 1, \cdots, N-1$. Let us denote $\mathscr{G}(t^{n+1}, t^n, \hat{y})$ and $\mathscr{F}(t^{n+1}, t^n, \hat{y})$ as the approximation to $y(t^{n+1})$ with the initial value $\hat{y} \approx y(t^n)$ through the propagator $\mathscr{G}$ and $\mathscr{F}$ respectively. The first step of parareal method is to compute an approximation in serial, i.e.,

$$y_1^{n+1} := \mathscr{G}(t^{n+1}, t^n, y_1^n),$$

with the initial value $y_1^0 = y(0)$. Once each processor P_n obtains the value y_1^n, they can compute $\mathscr{F}(t^{n+1}, t^n, y_1^n)$ in parallel, which is a more accurate approximation of $y(t^{n+1})$. The last step of the parareal method is a serial correction step

$$y_{k+1}^{n+1} := \mathscr{G}(t^{n+1}, t^n, y_{k+1}^n) + \mathscr{F}(t^{n+1}, t^n, y_k^n) - \mathscr{G}(t^{n+1}, t^n, y_k^n), \quad n = 0, 1, \cdots, N-1, \tag{1}$$

where the subscript k refers to the iteration number. Since the $\mathscr{F}$ provides the overall accuracy of parareal method [33,34], the iterative process (1) provides a converging sequence toward $y^{n+1} = \mathscr{F}(t^{n+1}, t^n, y^n)$.

Since the parareal method was proposed, it has sparked renewed interest in the construction of time parallel methods [36–41]. At the same time, these numerical methods which are more suitable for high-performance parallel computers can provide the new algorithm tools and theoretical basis for large-scale numerical simulations in practical applications. In this paper, we propose a time parallel decoupled algorithm for the Stokes/Darcy model through combining the decoupled method with parareal method together. This scheme aims to improve the computational efficiency through reducing the computing scale and improving the utilization rate of parallel computing resources. From another perspective, our algorithm can be viewed as an extension of a time-parallel algorithm in [42], which improves the parallel effectiveness through utilizing the decoupled techniques. Our scheme not only achieves the parallelism in temporal direction, but also enables the parallel computations of two decoupled subproblems at each time step due to the independence of the decoupled subproblems. Furthermore, we implement the spectral deferred correction (SDC) method [43–45] to improve the accuracy. Since parareal and SDC method both belong to the predictor-corrector methods, they can be well combined together to improve the computational efficiency and accuracy while ensuring the stability of discrete algorithms.

The outline of this paper is as follows. In section 2, the non-stationary mixed Stokes/Darcy model is provided with its weak formulation and properties. Section 3 is devoted to introduce our second-order time parallel decoupled algorithm. Section 4 demonstrates the stability of our scheme, while section 5 deduces its convergence. Section 6 includes three numerical tests that validate our theoretical analysis and demonstrate the accuracy, stability and efficiency of our algorithm.

2. The mixed Stokes/Darcy model

We consider the non-stationary mixed Stokes/Darcy model in a bounded domain $\Omega \subset \mathbb{R}^d$ ($d = 2$ or 3), which consists of the fluid flow domain Ω_f and the porous media region Ω_p. And two regions are separated by the interface $\Gamma = \overline{\Omega}_f \cap \overline{\Omega}_p$. Let us define $\Gamma_f = \partial\Omega_f \backslash \Gamma$ and $\Gamma_p = \partial\Omega_p \backslash \Gamma$.

Let $T > 0$ be a finite time. The motion of fluid flow in Ω_f is governed by the Stokes equations for the fluid velocity $\boldsymbol{u}$ and kinematic pressure p: $\forall t \in (0, T]$,

$$\begin{cases} \boldsymbol{u}_t - \nu\Delta\boldsymbol{u} + \nabla p = \boldsymbol{f}_1, & \text{in } \Omega_f \times (0, T], \quad (2) \\ \nabla \cdot \boldsymbol{u} = 0, & \text{in } \Omega_f \times (0, T], \quad (3) \\ \boldsymbol{u}(\boldsymbol{x}, 0) = \boldsymbol{u}^0(\boldsymbol{x}), & \text{in } \Omega_f, \quad (4) \\ \boldsymbol{u} = \boldsymbol{0}, & \text{on } \Gamma_f \times (0, T], \quad (5) \end{cases}$$

where $\nu > 0$ is the kinematic viscosity and $\boldsymbol{f}_1$ is the external force.

The motion of porous media flow in Ω_p is governed by the following equations for the piezometric head φ:

$$\begin{cases} S_0\varphi_t - \nabla \cdot \boldsymbol{u}_p = f_2, & \text{in } \Omega_p \times (0, T], \quad (6) \\ \boldsymbol{u}_p = -\boldsymbol{K}\nabla\varphi, & \text{in } \Omega_p \times (0, T], \quad (7) \\ \varphi(\boldsymbol{x}, 0) = \varphi^0(\boldsymbol{x}), & \text{in } \Omega_p, \quad (8) \\ \varphi = 0, & \text{on } \Gamma_p \times (0, T], \quad (9) \end{cases}$$

where $\boldsymbol{u}_p$ is the fluid velocity in Ω_p, S_0 is the specific mass storativity coefficient, $\boldsymbol{K}$ represents the hydraulic conductivity tensor, and f_2 is the source term. Indeed, combining the Darcy's law (7) with the continuity equation (6), we obtain the Darcy equation in $\Omega_p \times (0, T]$:

$$S_0\varphi_t - \nabla \cdot (\boldsymbol{K}\nabla\varphi) = f_2. \tag{10}$$

We consider the following interface conditions on $\Gamma \times (0,T]$:

$$\boldsymbol{u}\cdot\boldsymbol{n}_f - \boldsymbol{K}\nabla\varphi\cdot\boldsymbol{n}_p = 0, \tag{11}$$

$$p - \nu\boldsymbol{n}_f\frac{\partial\boldsymbol{u}}{\partial\boldsymbol{n}_f} = g\varphi, \tag{12}$$

$$-\nu\boldsymbol{\tau}_i\frac{\partial\boldsymbol{u}}{\partial\boldsymbol{n}_f} = \frac{\alpha\sqrt{\nu g}}{\sqrt{\mathrm{tr}(\boldsymbol{K})}}\boldsymbol{u}\cdot\boldsymbol{\tau}_i, \quad i=1,\cdots,d-1, \tag{13}$$

where $\boldsymbol{n}_f$ and $\boldsymbol{n}_p$ are the unit outward normal vectors on $\partial\Omega_f$ and $\partial\Omega_p$, g is the gravitational acceleration, $\{\boldsymbol{\tau}_i\}_{i=1}^{d-1}$ are the linearly independent unit tangential vectors on the interface Γ, and α is a positive parameter generally determined by experiments. These interface conditions represent the conservation of mass (11), the balance of normal forces (12) and the Beavers-Joseph-Saffman interface condition (13) across the interface Γ.

Let us denote $Q = L^2(\Omega_f)$ and

$$\boldsymbol{W}_f = \left\{\boldsymbol{v}\in\left(H^1(\Omega_f)\right)^d : \boldsymbol{v}|_{\Gamma_f} = \boldsymbol{0}\right\},$$
$$W_p = \left\{\psi\in H^1(\Omega_p) : \psi|_{\Gamma_p} = 0\right\}.$$

So we define the space $\boldsymbol{W} = \boldsymbol{W}_f\times W_p$, which is equipped with the norms as follows: $\forall\underline{\boldsymbol{z}} = (\boldsymbol{v},\psi)\in\boldsymbol{W}$,

$$\begin{aligned}
\|\underline{\boldsymbol{z}}\|_0 &= \sqrt{(\boldsymbol{v},\boldsymbol{v})_{\Omega_f} + gS_0(\psi,\psi)_{\Omega_p}},\\
\|\underline{\boldsymbol{z}}\|_W &= \sqrt{\nu(\nabla\boldsymbol{v},\nabla\boldsymbol{v})_{\Omega_f} + g(\boldsymbol{K}\nabla\psi,\nabla\psi)_{\Omega_p}}.
\end{aligned} \tag{14}$$

Here and afterwards, let us denote $(\cdot,\cdot)_D$ as the scalar product and $\|\cdot\|_{L^2(D)}$ as the L^2-norm in the region D for $D = \Omega_f$ or Ω_p.

The weak formulation of the non-stationary mixed Stokes/Darcy model (2)-(5), (8)-(13) is given as follows: for $\boldsymbol{f}_1\in L^2\left(0,T;L^2(\Omega_f)^d\right)$ and $f_2\in L^2\left(0,T;L^2(\Omega_p)\right)$, find $\underline{\boldsymbol{w}} = (\boldsymbol{u},\varphi)\in\left(L^\infty(0,T;L^2(\Omega_f))^d\cap L^2(0,T;\boldsymbol{W}_f)\right)\times\left(L^\infty(0,T;L^2(\Omega_p))\cap L^2(0,T;W_p)\right)$ and $p\in L^2(0,T;Q)$, such that $\forall\underline{\boldsymbol{z}} = (\boldsymbol{v},\psi)\in\boldsymbol{W}$, $q\in Q$, $t\in(0,T]$,

$$\begin{cases}
[\underline{\boldsymbol{w}}_t,\underline{\boldsymbol{z}}] + a(\underline{\boldsymbol{w}},\underline{\boldsymbol{z}}) + a_\Gamma(\underline{\boldsymbol{w}},\underline{\boldsymbol{z}}) + b(\underline{\boldsymbol{z}},p) = (\boldsymbol{f},\underline{\boldsymbol{z}}),\\
b(\underline{\boldsymbol{w}},q) = 0,\\
\underline{\boldsymbol{w}}(\boldsymbol{x},0) = \underline{\boldsymbol{w}}^0(\boldsymbol{x}),
\end{cases} \tag{15}$$

where

$$\begin{aligned}
&[\underline{\boldsymbol{w}}_t,\underline{\boldsymbol{z}}] = \left(\boldsymbol{u}_t,\boldsymbol{v}\right)_{\Omega_f} + gS_0\left(\varphi_t,\psi\right)_{\Omega_p},\\
&a(\underline{\boldsymbol{w}},\underline{\boldsymbol{z}}) = a_f(\boldsymbol{u},\boldsymbol{v}) + a_p(\varphi,\psi),\\
&a_f(\boldsymbol{u},\boldsymbol{v}) = \nu\left(\nabla\boldsymbol{u},\nabla\boldsymbol{v}\right)_{\Omega_f} + \sum_{i=1}^{d-1}\int_\Gamma\frac{\alpha\sqrt{\nu g}}{\sqrt{\mathrm{tr}(\boldsymbol{K})}}\left(\boldsymbol{u}\cdot\boldsymbol{\tau}_i\right)\left(\boldsymbol{v}\cdot\boldsymbol{\tau}_i\right),\\
&a_p(\varphi,\psi) = g\left(\boldsymbol{K}\nabla\varphi,\nabla\psi\right)_{\Omega_p},\\
&a_\Gamma(\underline{\boldsymbol{w}},\underline{\boldsymbol{z}}) = g\left(\varphi,\boldsymbol{v}\cdot\boldsymbol{n}_f\right)_{L^2(\Gamma)} - g\left(\psi,\boldsymbol{u}\cdot\boldsymbol{n}_f\right)_{L^2(\Gamma)} = g\int_\Gamma\left(\varphi\boldsymbol{v}\cdot\boldsymbol{n}_f - \psi\boldsymbol{u}\cdot\boldsymbol{n}_f\right),\\
&b(\underline{\boldsymbol{z}},p) \equiv b(\boldsymbol{v},p) = -(p,\nabla\cdot\boldsymbol{v})_{\Omega_f},\\
&(\boldsymbol{f},\underline{\boldsymbol{z}}) = \left(\boldsymbol{f}_1,\boldsymbol{v}\right)_{\Omega_f} + g\left(f_2,\psi\right)_{\Omega_p},\\
&\underline{\boldsymbol{w}}^0(\boldsymbol{x}) = \left(\boldsymbol{u}^0(\boldsymbol{x}),\varphi^0(\boldsymbol{x})\right).
\end{aligned}$$

It is known that $a_f(\cdot,\cdot)$ and $a_p(\cdot,\cdot)$ are symmetric. And $a_\Gamma(\cdot,\cdot)$ satisfies the following properties: $\forall\underline{\boldsymbol{w}},\underline{\boldsymbol{z}}\in\boldsymbol{W}$

$$a_\Gamma(\underline{\boldsymbol{w}},\underline{\boldsymbol{z}}) = -a_\Gamma(\underline{\boldsymbol{z}},\underline{\boldsymbol{w}}) \quad\text{and}\quad a_\Gamma(\underline{\boldsymbol{w}},\underline{\boldsymbol{w}}) = 0. \tag{16}$$

Furthermore, for the hydraulic conductivity tensor $\boldsymbol{K}$ in (10), we assume that: $\exists\ k_{\min},k_{\max}>0$, such that

$$k_{\min}|x|^2 \le \boldsymbol{K}\boldsymbol{x}\cdot\boldsymbol{x} \le k_{\max}|\boldsymbol{x}|^2 \quad \text{a.e.}\ \ \boldsymbol{x}\in\Omega_p. \tag{17}$$

From (17), we have

$$\frac{1}{\sqrt{k_{\max}}}\left\|\boldsymbol{K}^{\frac12}\nabla\psi\right\|_{\Omega_p} \le \|\nabla\psi\|_{\Omega_p} \le \frac{1}{\sqrt{k_{\min}}}\left\|\boldsymbol{K}^{\frac12}\nabla\psi\right\|_{\Omega_p}, \quad \forall\psi\in W_p. \tag{18}$$

Last, let us recall the Poincaré and trace inequalities that are useful in our analysis: there exist constants C_p and C_t, which only depend on the region Ω_f, such that $\forall\boldsymbol{v}\in\boldsymbol{W}_f$,

$$\|\boldsymbol{v}\|_{\Omega_f} \le C_p\|\nabla\boldsymbol{v}\|_{\Omega_f}, \qquad \|\boldsymbol{v}\|_{L^2(\Gamma)} \le C_t\|\boldsymbol{v}\|_{\Omega_f}^{\frac12}\|\nabla\boldsymbol{v}\|_{\Omega_f}^{\frac12}, \tag{19}$$

and there exist constants $\tilde{C}_p$ and $\tilde{C}_t$, which only depend on the region Ω_p, such that $\forall\psi \in W_p$,

$$\|\psi\|_{\Omega_p} \le \tilde{C}_p \|\nabla\psi\|_{\Omega_p}, \qquad \|\psi\|_{L^2(\Gamma)} \le \tilde{C}_t \|\psi\|^{\frac{1}{2}}_{\Omega_p} \|\nabla\psi\|^{\frac{1}{2}}_{\Omega_p}. \tag{20}$$

3. Numerical algorithms

Now we present the second-order time parallel decoupled algorithm for the mixed Stokes/Darcy model, where the finite element method is used for the spatial discretization, as well as the parareal and SDC methods are used for the temporal discretization. Since the parareal method belongs to the predictor-corrector schemes, we need to provide a first-order decoupled scheme as the predictor. Then by utilizing the decoupled approach and the SDC strategy, we construct the corrector and achieve the ultimate second-order time-parallel decoupled algorithm.

For the spatial discretization, we consider the quasi-uniform triangulation $\mathcal{T}^h = \mathcal{T}_f^h \bigcup \mathcal{T}_p^h$ of the domain $\overline{\Omega} = \overline{\Omega}_f \cap \overline{\Omega}_p$, which depends on the mesh size $h > 0$. And the triangulations $\mathcal{T}_f^h$ and $\mathcal{T}_f^h$ induced on the regions Ω_f and Ω_p are required to be compatible on the interface Γ. We choose the finite element spaces $\boldsymbol{W}_{f,h} \subset \boldsymbol{W}_f$, $W_{p,h} \subset W_p$ and $Q_h \subset Q$. Define $\boldsymbol{W}_h = \boldsymbol{W}_{f,h} \times W_{p,h} \subset \boldsymbol{W}$, and assume that $\boldsymbol{W}_{f,h}$ and Q_h satisfy the discrete inf-sup condition.

Let us define a linear projection operator (see [21]) $P_h = (P_h^w, P_h^p)$ from $\boldsymbol{W} \times Q$ onto $\boldsymbol{W}_h \times Q_h$: $\forall t \in [0,T]$, $\left(\underline{\boldsymbol{w}}(t), p(t)\right) \in \boldsymbol{W} \times Q$,

$$\begin{cases} a\left(P_h^w \underline{\boldsymbol{w}}(t) - \underline{\boldsymbol{w}}(t), \underline{\boldsymbol{z}}_h\right) + a_\Gamma\left(P_h^w \underline{\boldsymbol{w}}(t) - \underline{\boldsymbol{w}}(t), \underline{\boldsymbol{z}}_h\right) + b\left(\underline{\boldsymbol{z}}_h, P_h^p p(t) - p(t)\right) = 0, \quad \forall \underline{\boldsymbol{z}}_h \in \boldsymbol{W}_h. \\ b\left(P_h^w \underline{\boldsymbol{w}}(t), q_h\right) = 0, \quad \forall q_h \in Q_h. \end{cases} \tag{21}$$

Indeed, under the certain smoothing assumptions on the exact solutions, we have the following error estimates: for $k, l > 1, s > 0$,

$$\begin{aligned} &\left\|(P_h^w - I)\underline{\boldsymbol{w}}(t)\right\|_0 \le C\left(h^k \|\boldsymbol{u}(t)\|_{H^k(\Omega_f)} + h^l \|\varphi(t)\|_{H^l(\Omega_p)}\right), \\ &\left\|(P_h^p - I)p(t)\right\|_{\Omega_f} \le C h^s \|p(t)\|_{H^s(\Omega_f)}, \\ &\left\|(P_h^w - I)\underline{\boldsymbol{w}}(t)\right\|_W \le C\left(h^{k-1} \|\boldsymbol{u}(t)\|_{H^k(\Omega_f)} + h^{l-1} \|\varphi(t)\|_{H^l(\Omega_p)}\right), \end{aligned} \tag{22}$$

where I denotes the identity operator, and the constant $C > 0$ varies across different locations but remains unaffected by the mesh size and time step.

Without loss of generality, let us assume a uniform mesh applied to the time interval $[0,T]$ with $t^n = n\Delta t, n = 0, 1, \cdots, N-1$, where $\Delta t = T/N > 0$ is a time step. So that, we decompose this time interval into N subintervals $[t^n, t^{n+1}]$, $n = 0, 1, \cdots, N-1$, and we utilize the superscripts to represent the time levels in this paper. In the general strategy of parareal method, the N subintervals $[t^n, t^{n+1}](n = 0, 1, \cdots, N-1)$ are assigned to different processors, so we assume there are N processors and denote by $P_1, P_2, \cdots, P_N$. Since the purpose of this paper is to construct a second-order time parallel decoupled algorithm for the Stokes/Darcy problem, we apply the first-order decoupled method [21] as $\mathscr{G}$ and a second-order SDC sweep [42,43] as $\mathscr{F}$. Let $\left(\underline{\boldsymbol{w}}_{1,h}^{n+1}, p_{1,h}^{n+1}\right)$ denote the approximate solutions by the first-order decoupled scheme, in which a decoupling approach is proposed based on the interface approximation via temporal extrapolation. And let us denote $\left(\underline{\boldsymbol{w}}_{2,h}^{n+1}, p_{2,h}^{n+1}\right)$ as the approximate solutions by the second-order time-parallel decoupled schemes to the exact solution $\left(\boldsymbol{u}(t^{n+1}), \varphi(t^{n+1}), p(t^{n+1})\right)$. Note that when we simultaneously compute $\mathscr{F}(t^{n+1}, t^n, \underline{\boldsymbol{w}}_{1,h}^n)$ over each subinterval $[t^n, t^{n+1}]$, $n = 0, 1, \cdots, N-1$, the interface terms are treated explicitly to achieve decoupling. Specially, the approximation solution at time t^{n+1} obtained in the previous step (i.e. $\underline{\boldsymbol{w}}_{1,h}^{n+1}$) is used to explicitly process interface terms in the second step of parareal emthod. It is worth mentioning that the convergence order of parareal method [33] is decided by the order of the $\mathscr{G}$ propagator and the number of iterations. Because we choose a first-order numerical method as $\mathscr{G}$, the convergence order in time will increase by one time with each iteration. Since we want to create a second-order algorithm for the Stokes/Darcy model, two iterations are sufficient for our algorithm. Next, we denote our scheme as the Para-SDC decoupled algorithm for short. Based on the framework of parareal method, now we present the specific steps of Para-SDC decoupled schemes for the unsteady mixed Stokes/Darcy model in Algorithm 3.1, and these three steps are named the serial prediction step, the parallel correction step and the serial correction step respectively.

Algorithm 3.1. *(Para-SDC decoupled algorithm for the Stokes/Darcy model)*

Step 1. Serial Prediction Step : *Compute* $\mathscr{G}(t^{n+1}, t^n, \underline{\boldsymbol{w}}_{1,h}^n) := \left(\underline{\boldsymbol{w}}_{1,h}^{n+1}, p_{1,h}^{n+1}\right)$ *with* $n = 0, \ldots, N-1$ *in serial: find* $\left(\underline{\boldsymbol{w}}_{1,h}^{n+1}, p_{1,h}^{n+1}\right) \in \boldsymbol{W}_h \times Q_h$*, such that* $\forall \left(\underline{\boldsymbol{z}}_h, q_h\right) \in \boldsymbol{W}_h \times Q_h$,

$$\begin{cases} \left[\dfrac{\underline{\boldsymbol{w}}_{1,h}^{n+1} - \underline{\boldsymbol{w}}_{1,h}^n}{\Delta t}, \underline{\boldsymbol{z}}_h\right] + a\left(\underline{\boldsymbol{w}}_{1,h}^{n+1}, \underline{\boldsymbol{z}}_h\right) + b\left(\underline{\boldsymbol{z}}_h, p_{1,h}^{n+1}\right) = -a_\Gamma\left(\underline{\boldsymbol{w}}_{1,h}^n, \underline{\boldsymbol{z}}_h\right) + \left(\boldsymbol{f}^{n+1}, \underline{\boldsymbol{z}}_h\right), \\ b\left(\underline{\boldsymbol{w}}_{1,h}^{n+1}, q_h\right) = 0, \\ \underline{\boldsymbol{w}}_{1,h}^0 = P_h^w \underline{\boldsymbol{w}}^0. \end{cases} \tag{23}$$

Step 2. Parallel Correction Step : *Compute* $\mathscr{F}(t^{n+1}, t^n, \underline{\boldsymbol{w}}_{1,h}^n) := \left(\underline{\boldsymbol{w}}_F^{n+1}, p_F^{n+1}\right)$ *with* $n = 0, \ldots, N-1$ *simultaneously. Let us take the example of processor* P_n *over the sub-interval* $[t^n, t^{n+1}]$*: find* $\left(\underline{\boldsymbol{w}}_F^{n+1}, p_F^{n+1}\right) \in \boldsymbol{W}_h \times Q_h$*, such that* $\forall \left(\underline{\boldsymbol{z}}_h, q_h\right) \in \boldsymbol{W}_h \times Q_h$,

$$\begin{cases} \left[\dfrac{\underline{\boldsymbol{w}}_F^{n+1}-\underline{\boldsymbol{w}}_{1,h}^n}{\Delta t},\underline{\boldsymbol{z}}_h\right]+a\left(\underline{\boldsymbol{w}}_F^{n+1},\underline{\boldsymbol{z}}_h\right)+b\left(\underline{\boldsymbol{z}}_h,p_F^{n+1}\right) \\ \quad =-a_\Gamma\left(\underline{\boldsymbol{w}}_{1,h}^{n+1},\underline{\boldsymbol{z}}_h\right)+a\left(\dfrac{\underline{\boldsymbol{w}}_{1,h}^{n+1}-\underline{\boldsymbol{w}}_{1,h}^n}{2},\underline{\boldsymbol{z}}_h\right)+a_\Gamma\left(\dfrac{\underline{\boldsymbol{w}}_{1,h}^{n+1}-\underline{\boldsymbol{w}}_{1,h}^n}{2},\underline{\boldsymbol{z}}_h\right)+b\left(\underline{\boldsymbol{z}}_h,\dfrac{p_{1,h}^{n+1}-p_{1,h}^n}{2}\right)+\left(\dfrac{\boldsymbol{f}^{n+1}+\boldsymbol{f}^n}{2},\underline{\boldsymbol{z}}_h\right), \\ b\left(\underline{\boldsymbol{w}}_F^{n+1},q_h\right)=0. \end{cases} \tag{24}$$

Step 3. Serial Correction Step : *Compute* $\mathscr{G}(t^{n+1},t^n,\underline{\boldsymbol{w}}_{2,h}^n):=\left(\underline{\boldsymbol{w}}_G^{n+1},p_G^{n+1}\right)$ *with* $n=0,\dots,N-1$ *in serial: find* $\left(\underline{\boldsymbol{w}}_G^{n+1},p_G^{n+1}\right)\in\boldsymbol{W}_h\times Q_h$*, such that* $\forall\left(\underline{\boldsymbol{z}}_h,q_h\right)\in\boldsymbol{W}_h\times Q_h$,

$$\begin{cases} \left[\dfrac{\underline{\boldsymbol{w}}_G^{n+1}-\underline{\boldsymbol{w}}_{2,h}^n}{\Delta t},\underline{\boldsymbol{z}}_h\right]+a\left(\underline{\boldsymbol{w}}_G^{n+1},\underline{\boldsymbol{z}}_h\right)+b\left(\underline{\boldsymbol{z}}_h,p_G^{n+1}\right)=-a_\Gamma\left(\underline{\boldsymbol{w}}_{2,h}^n,\underline{\boldsymbol{z}}_h\right)+\left(\boldsymbol{f}^{n+1},\underline{\boldsymbol{z}}_h\right), \\ b\left(\underline{\boldsymbol{w}}_G^{n+1},q_h\right)=0. \end{cases} \tag{25}$$

Then with the initial value $\underline{\boldsymbol{w}}_{2,h}^0=P_h^w\underline{\boldsymbol{w}}^0$*, we get*

$$\begin{cases} \underline{\boldsymbol{w}}_{2,h}^{n+1}:=\underline{\boldsymbol{w}}_G^{n+1}+\underline{\boldsymbol{w}}_F^{n+1}-\underline{\boldsymbol{w}}_{1,h}^{n+1}, \\ p_{2,h}^{n+1}:=p_G^{n+1}+p_F^{n+1}-p_{1,h}^{n+1}. \end{cases} \tag{26}$$

It is easy to see that each of the discrete models from (23), (24) and (25), can be equivalent to two decoupled problems with associated boundary conditions defined by the known numerical solutions from the previous steps or the previous time level on the interface Γ. The decoupled equations corresponding to (23) have been given in [21] and the same processes can be applied to the discrete equation (25). Therefore, we only decompose the relatively complex equation (24) into a Stokes subproblem in Ω_f and a Darcy subproblem in Ω_p as follows. The decoupled Stokes equations in Ω_f read: find $\left(\boldsymbol{u}_F^{n+1},p_F^{n+1}\right)\in\boldsymbol{W}_{f,h}\times Q_h$ with $n=0,1,\dots,N-1$, such that $\forall\underline{\boldsymbol{z}}_h\in\boldsymbol{W}_h$ and $q_h\in Q_h$,

$$\begin{cases} \left(\dfrac{\boldsymbol{u}_F^{n+1}-\boldsymbol{u}_{1,h}^n}{\Delta t},\boldsymbol{v}_h\right)+a_f\left(\boldsymbol{u}_F^{n+1},\boldsymbol{v}_h\right)+b\left(\boldsymbol{v}_h,p_F^{n+1}\right) \\ \quad =-g\displaystyle\int_\Gamma\varphi_{1,h}^{n+1}\boldsymbol{v}_h\cdot\boldsymbol{n}_f+a_f\left(\dfrac{\boldsymbol{u}_{1,h}^{n+1}-\boldsymbol{u}_{1,h}^n}{2},\boldsymbol{v}_h\right)+g\displaystyle\int_\Gamma\dfrac{\varphi_{1,h}^{n+1}-\varphi_{1,h}^n}{2}\boldsymbol{v}_h\cdot\boldsymbol{n}_f+b\left(\boldsymbol{v}_h,\dfrac{p_{1,h}^{n+1}-p_{1,h}^n}{2}\right)+\left(\dfrac{\boldsymbol{f}_1^{n+1}+\boldsymbol{f}_1^n}{2},\boldsymbol{v}_h\right)_{\Omega_f}, \\ b\left(\boldsymbol{u}_F^{n+1},q_h\right)=0, \end{cases} \tag{27}$$

and the discrete Darcy equations in Ω_p read: find $\varphi_F^{n+1}\in W_{p,h}$ with $n=0,1,\dots,N-1$, such that $\forall\psi_h\in W_{p,h}$,

$$\begin{aligned} &gS_0\left(\dfrac{\varphi_F^{n+1}-\varphi_{1,h}^n}{\Delta t},\psi_h\right)+a_p\left(\varphi_F^{n+1},\psi_h\right) \\ &=g\int_\Gamma\psi_h\boldsymbol{u}_{1,h}^{n+1}\cdot\boldsymbol{n}_f+a_p\left(\dfrac{\varphi_{1,h}^{n+1}-\varphi_{1,h}^n}{2},\psi_h\right)-g\int_\Gamma\psi_h\dfrac{\boldsymbol{u}_{1,h}^{n+1}-\boldsymbol{u}_{1,h}^n}{2}\cdot\boldsymbol{n}_f+g\left(\dfrac{f_2^{n+1}+f_2^n}{2},\psi_h\right)_{\Omega_p}. \end{aligned} \tag{28}$$

It is worth mentioning that the discrete schemes (27) and (28) are independent to each other. Therefore, if there are two processors assigned over each time step, we can solve these two independent problems concurrently. This conclusion is also applicable to the decoupled equations (23) and (25). So that it can further improve the computational efficiency of our algorithm.

4. The stability analysis

In this section, we mainly focus on the stability of the second-order Para-SDC decoupled scheme (Algorithm 3.1), which will be presented under a time step restriction. Lemma 4.1 presents several estimations of the interface term $a_\Gamma(\cdot,\cdot)$, which will be employed in the later analysis.

Lemma 4.1. *[21,22] There exist* $C_1=C_t^2\tilde{C}_t^2$ *and* $C_2=C_p\tilde{C}_p$*, such that* $\forall\underline{\boldsymbol{w}},\underline{\boldsymbol{z}}\in\boldsymbol{W}$, $\varepsilon>0$,

$$|a_\Gamma(\underline{\boldsymbol{w}},\underline{\boldsymbol{z}})|\le\varepsilon\|\underline{\boldsymbol{w}}\|_W^2+\frac{gC_1C_2}{4\varepsilon\nu k_{\min}}\|\underline{\boldsymbol{z}}\|_W^2, \tag{29}$$

and

$$|a_\Gamma(\underline{\boldsymbol{w}},\underline{\boldsymbol{z}})|\le\varepsilon\left(\|\underline{\boldsymbol{w}}\|_W^2+\|\underline{\boldsymbol{z}}\|_W^2\right)+\frac{gC_1}{16\varepsilon\sqrt{\nu S_0}k_{\min}}\left(\|\underline{\boldsymbol{w}}\|_0^2+\|\underline{\boldsymbol{z}}\|_0^2\right). \tag{30}$$

Moreover, for all $\underline{\boldsymbol{w}}_h$, $\underline{\boldsymbol{z}}_h\in\boldsymbol{W}_h$,

$$|a_\Gamma(\underline{\boldsymbol{w}}_h,\underline{\boldsymbol{z}}_h)|\le\varepsilon\|\underline{\boldsymbol{w}}_h\|_W^2+\frac{gC_1}{4\varepsilon h}\max\left\{\frac{\tilde{C}_pC_I}{k_{\min}},\frac{C_p\tilde{C}_I}{\nu S_0}\right\}\|\underline{\boldsymbol{z}}_h\|_0^2. \tag{31}$$

Next, we provide the stability of the first-order decoupled scheme (23) in the following lemma.

Lemma 4.2. *Assume that the time step size Δt satisfies the condition*

$$\frac{4gC_1}{\sqrt{\nu S_0 k_{\min}}}\Delta t < 1, \tag{32}$$

and denote $\kappa_1 = \frac{2gC_1}{\sqrt{\nu S_0 k_{\min}}}$. Then we have

$$\begin{aligned}&\|\underline{\boldsymbol{w}}_{1,h}^{m}\|_0^2 + \Delta t\sum_{n=0}^{m}\|\underline{\boldsymbol{w}}_{1,h}^{n}\|_W^2\\ &\le \exp\left(\Delta t\sum_{n=0}^{m}\frac{\kappa_1}{1-\Delta t\kappa_1}\right)\left(2\|\underline{\boldsymbol{w}}^0\|_0^2 + 2\Delta t\|\underline{\boldsymbol{w}}^0\|_W^2 + \frac{4C_p^2}{\nu}\Delta t\sum_{n=0}^{m-1}\|\boldsymbol{f}_1^{n+1}\|_{\Omega_f}^2 + \frac{4g\tilde{C}_p^2}{k_{\min}}\Delta t\sum_{n=0}^{m-1}\|f_2^{n+1}\|_{\Omega_p}^2\right).\end{aligned} \tag{33}$$

Proof. Taking $\underline{\boldsymbol{z}}_h = 2\Delta t\underline{\boldsymbol{w}}_{1,h}^{n+1}$ and $q_h = p_{1,h}^{n+1}$ in (23), using the divergence-free property and the elementary identity

$$2a\cdot(a-b) = |a|^2 - |b|^2 + |a-b|^2, \quad \forall a, b\in\mathbb{R} \text{ or } \mathbb{R}^d,$$

we have

$$\begin{aligned}&\|\underline{\boldsymbol{w}}_{1,h}^{n+1}\|_0^2 - \|\underline{\boldsymbol{w}}_{1,h}^{n}\|_0^2 + \|\underline{\boldsymbol{w}}_{1,h}^{n+1} - \underline{\boldsymbol{w}}_{1,h}^{n}\|_0^2 + 2\Delta t\|\underline{\boldsymbol{w}}_{1,h}^{n+1}\|_W^2 + 2\Delta t\sum_{i=1}^{d-1}\frac{\alpha\sqrt{\nu g}}{\sqrt{\mathrm{tr}(\boldsymbol{K})}}\|\boldsymbol{w}_{1,h}^{n+1}\cdot\tau_i\|_{L^2(\Gamma)}^2\\ &= -2\Delta t a_\Gamma(\underline{\boldsymbol{w}}_{1,h}^{n}, \underline{\boldsymbol{w}}_{1,h}^{n+1}) + 2\Delta t(\boldsymbol{f}^{n+1}, \underline{\boldsymbol{w}}_{1,h}^{n+1}).\end{aligned} \tag{34}$$

To estimate the first term on the right hand side of (34), applying (16) and (30), we have

$$\begin{aligned}&-2\Delta t a_\Gamma(\underline{\boldsymbol{w}}_{1,h}^{n}, \underline{\boldsymbol{w}}_{1,h}^{n+1}) = 2\Delta t a_\Gamma(\underline{\boldsymbol{w}}_{1,h}^{n+1}, \underline{\boldsymbol{w}}_{1,h}^{n})\\ &\le \varepsilon\Delta t\left(\|\underline{\boldsymbol{w}}_{1,h}^{n+1}\|_W^2 + \|\underline{\boldsymbol{w}}_{1,h}^{n}\|_W^2\right) + \frac{gC_1}{4\varepsilon\sqrt{\nu S_0 k_{\min}}}\Delta t\left(\|\underline{\boldsymbol{w}}_{1,h}^{n+1}\|_0^2 + \|\underline{\boldsymbol{w}}_{1,h}^{n}\|_0^2\right).\end{aligned} \tag{35}$$

Utilizing the Hölder and Poincaré inequalities along with the Young's inequality

$$ab \le \varepsilon a^2 + \frac{1}{4\varepsilon}b^2, \quad a, b > 0, \ \varepsilon > 0,$$

and considering (18), we get

$$\begin{aligned}2\Delta t(\boldsymbol{f}^{n+1}, \underline{\boldsymbol{w}}_{1,h}^{n+1}) &= 2\Delta t(\boldsymbol{f}_1^{n+1}, \boldsymbol{u}_{1,h}^{n+1})_{\Omega_f} + 2\Delta t g(f_2^{n+1}, \varphi_{1,h}^{n+1})_{\Omega_p}\\ &\le 2\Delta t\|\boldsymbol{f}_1^{n+1}\|_{\Omega_f}\|\boldsymbol{u}_{1,h}^{n+1}\|_{\Omega_f} + 2\Delta t g\|f_2^{n+1}\|_{\Omega_p}\|\varphi_{1,h}^{n+1}\|_{\Omega_p}\\ &\le 2\Delta t C_p\|\boldsymbol{f}_1^{n+1}\|_{\Omega_f}\|\nabla\boldsymbol{u}_{1,h}^{n+1}\|_{\Omega_f} + 2\Delta t g\tilde{C}_p\|f_2^{n+1}\|_{\Omega_p}\|\nabla\varphi_{1,h}^{n+1}\|_{\Omega_p}\\ &\le \varepsilon\nu\Delta t\|\nabla\boldsymbol{u}_{1,h}^{n+1}\|_{\Omega_f}^2 + \frac{C_p^2}{\varepsilon\nu}\Delta t\|\boldsymbol{f}_1^{n+1}\|_{\Omega_f}^2 + \varepsilon g k_{\min}\Delta t\|\nabla\varphi_{1,h}^{n+1}\|_{\Omega_p}^2 + \frac{g\tilde{C}_p^2}{\varepsilon k_{\min}}\Delta t\|f_2^{n+1}\|_{\Omega_p}^2\\ &\le \varepsilon\nu\Delta t\|\nabla\boldsymbol{u}_{1,h}^{n+1}\|_{\Omega_f}^2 + \varepsilon g\Delta t\|\boldsymbol{K}^{\frac{1}{2}}\nabla\varphi_{1,h}^{n+1}\|_{\Omega_p}^2 + \frac{C_p^2}{\varepsilon\nu}\Delta t\|\boldsymbol{f}_1^{n+1}\|_{\Omega_f}^2 + \frac{g\tilde{C}_p^2}{\varepsilon k_{\min}}\Delta t\|f_2^{n+1}\|_{\Omega_p}^2\\ &\le \varepsilon\Delta t\|\underline{\boldsymbol{w}}_{1,h}^{n+1}\|_W^2 + \frac{C_p^2}{\varepsilon\nu}\Delta t\|\boldsymbol{f}_1^{n+1}\|_{\Omega_f}^2 + \frac{g\tilde{C}_p^2}{\varepsilon k_{\min}}\Delta t\|f_2^{n+1}\|_{\Omega_p}^2.\end{aligned} \tag{36}$$

Replacing the bounds given by (35) and (36) into the relation (34), we can derive that

$$\begin{aligned}&\|\underline{\boldsymbol{w}}_{1,h}^{n+1}\|_0^2 - \|\underline{\boldsymbol{w}}_{1,h}^{n}\|_0^2 + \|\underline{\boldsymbol{w}}_{1,h}^{n+1} - \underline{\boldsymbol{w}}_{1,h}^{n}\|_0^2 + 2\Delta t\|\underline{\boldsymbol{w}}_{1,h}^{n+1}\|_W^2 + 2\Delta t\sum_{i=1}^{d-1}\frac{\alpha\sqrt{\nu g}}{\sqrt{\mathrm{tr}(\boldsymbol{K})}}\|\boldsymbol{w}_{1,h}^{n+1}\cdot\tau_i\|_{L^2(\Gamma)}^2\\ &\le 2\varepsilon\Delta t\|\underline{\boldsymbol{w}}_{1,h}^{n+1}\|_W^2 + \varepsilon\Delta t\|\underline{\boldsymbol{w}}_{1,h}^{n}\|_W^2 + \frac{gC_1}{4\varepsilon\sqrt{\nu S_0 k_{\min}}}\Delta t\left(\|\underline{\boldsymbol{w}}_{1,h}^{n+1}\|_0^2 + \|\underline{\boldsymbol{w}}_{1,h}^{n}\|_0^2\right) + \frac{C_p^2}{\varepsilon\nu}\Delta t\|\boldsymbol{f}_1^{n+1}\|_{\Omega_f}^2 + \frac{g\tilde{C}_p^2}{\varepsilon k_{\min}}\Delta t\|f_2^{n+1}\|_{\Omega_p}^2.\end{aligned} \tag{37}$$

Setting $\varepsilon = 1/2$ in (37) and omitting the non-negative term $2\Delta t\sum_{i=1}^{d-1}\frac{\alpha\sqrt{\nu g}}{\sqrt{\mathrm{tr}(\boldsymbol{K})}}\|\boldsymbol{w}_{1,h}^{n+1}\cdot\tau_i\|_{L^2(\Gamma)}^2$, we obtain

$$\begin{aligned}&\|\underline{\boldsymbol{w}}_{1,h}^{n+1}\|_0^2 - \|\underline{\boldsymbol{w}}_{1,h}^{n}\|_0^2 + \|\underline{\boldsymbol{w}}_{1,h}^{n+1} - \underline{\boldsymbol{w}}_{1,h}^{n}\|_0^2 + \Delta t\|\underline{\boldsymbol{w}}_{1,h}^{n+1}\|_W^2 - \frac{1}{2}\Delta t\|\underline{\boldsymbol{w}}_{1,h}^{n}\|_W^2\\ &\le \frac{gC_1}{2\sqrt{\nu S_0 k_{\min}}}\Delta t\left(\|\underline{\boldsymbol{w}}_{1,h}^{n+1}\|_0^2 + \|\underline{\boldsymbol{w}}_{1,h}^{n}\|_0^2\right) + \frac{2C_p^2}{\nu}\Delta t\|\boldsymbol{f}_1^{n+1}\|_{\Omega_f}^2 + \frac{2g\tilde{C}_p^2}{k_{\min}}\Delta t\|f_2^{n+1}\|_{\Omega_p}^2.\end{aligned}$$

Summing from $n = 0, \cdots, m-1$, a straightforward computation leads to

$$\|\underline{\boldsymbol{w}}_{1,h}^m\|_0^2+\sum_{n=0}^{m-1}\|\underline{\boldsymbol{w}}_{1,h}^{n+1}-\underline{\boldsymbol{w}}_{1,h}^n\|_0^2+\frac{1}{2}\Delta t\sum_{n=0}^{m-1}\|\underline{\boldsymbol{w}}_{1,h}^{n+1}\|_W^2+\frac{1}{2}\Delta t\|\underline{\boldsymbol{w}}_{1,h}^m\|_W^2$$
$$\leq\frac{gC_1}{\sqrt{\nu S_0k_{\min}}}\Delta t\sum_{n=0}^{m}\|\underline{\boldsymbol{w}}_{1,h}^n\|_0^2+\|\underline{\boldsymbol{w}}_{1,h}^0\|_0^2+\frac{1}{2}\Delta t\|\underline{\boldsymbol{w}}_{1,h}^0\|_W^2+\frac{2C_p^2}{\nu}\Delta t\sum_{n=0}^{m-1}\|\boldsymbol{f}_1^{n+1}\|_{\Omega_f}^2+\frac{2g\tilde{C}_p^2}{k_{\min}}\Delta t\sum_{n=0}^{m-1}\|f_2^{n+1}\|_{\Omega_p}^2.$$

This gives

$$\frac{1}{2}\|\underline{\boldsymbol{w}}_{1,h}^m\|_0^2+\frac{1}{2}\sum_{n=0}^{m-1}\|\underline{\boldsymbol{w}}_{1,h}^{n+1}-\underline{\boldsymbol{w}}_{1,h}^n\|_0^2+\frac{1}{2}\Delta t\sum_{n=0}^{m-1}\|\underline{\boldsymbol{w}}_{1,h}^{n+1}\|_W^2+\frac{1}{2}\Delta t\|\underline{\boldsymbol{w}}_{1,h}^m\|_W^2$$
$$\leq\frac{gC_1}{\sqrt{\nu S_0k_{\min}}}\Delta t\sum_{n=0}^{m}\|\underline{\boldsymbol{w}}_{1,h}^n\|_0^2+\|\underline{\boldsymbol{w}}_{1,h}^0\|_0^2+\frac{1}{2}\Delta t\|\underline{\boldsymbol{w}}_{1,h}^0\|_W^2+\frac{2C_p^2}{\nu}\Delta t\sum_{n=0}^{m-1}\|\boldsymbol{f}_1^{n+1}\|_{\Omega_f}^2+\frac{2g\tilde{C}_p^2}{k_{\min}}\Delta t\sum_{n=0}^{m-1}\|f_2^{n+1}\|_{\Omega_p}^2. \tag{38}$$

Next, adding the term $\frac{1}{2}\Delta t\|\underline{\boldsymbol{w}}_{1,h}^0\|_W^2$ to both sides of (38), omitting the non-negative term $\frac{1}{2}\Delta t\|\underline{\boldsymbol{w}}_{1,h}^m\|_W^2$, and multiplying both sides of the new relation by 2 yield

$$\|\underline{\boldsymbol{w}}_{1,h}^m\|_0^2+\sum_{n=0}^{m-1}\|\underline{\boldsymbol{w}}_{1,h}^{n+1}-\underline{\boldsymbol{w}}_{1,h}^n\|_0^2+\Delta t\sum_{n=0}^{m}\|\underline{\boldsymbol{w}}_{1,h}^{n}\|_W^2$$
$$\leq\frac{2gC_1}{\sqrt{\nu S_0k_{\min}}}\Delta t\sum_{n=0}^{m}\|\underline{\boldsymbol{w}}_{1,h}^n\|_0^2+2\|\underline{\boldsymbol{w}}_{1,h}^0\|_0^2+2\Delta t\|\underline{\boldsymbol{w}}_{1,h}^0\|_W^2+\frac{4C_p^2}{\nu}\Delta t\sum_{n=0}^{m-1}\|\boldsymbol{f}_1^{n+1}\|_{\Omega_f}^2+\frac{4g\tilde{C}_p^2}{k_{\min}}\Delta t\sum_{n=0}^{m-1}\|f_2^{n+1}\|_{\Omega_p}^2.$$

We choose the time step satisfies the condition (32). Then from the discrete Gronwall inequality, we derive

$$\|\underline{\boldsymbol{w}}_{1,h}^m\|_0^2+\Delta t\sum_{n=0}^{m}\|\underline{\boldsymbol{w}}_{1,h}^{n}\|_W^2$$
$$\leq\exp\left(\Delta t\sum_{n=0}^{m}\frac{\kappa_1}{1-\Delta t\kappa_1}\right)\left(2\|\underline{\boldsymbol{w}}_{1,h}^0\|_0^2+2\Delta t\|\underline{\boldsymbol{w}}_{1,h}^0\|_W^2+\frac{4C_p^2}{\nu}\Delta t\sum_{n=0}^{m-1}\|\boldsymbol{f}_1^{n+1}\|_{\Omega_f}^2+\frac{4g\tilde{C}_p^2}{k_{\min}}\Delta t\sum_{n=0}^{m-1}\|f_2^{n+1}\|_{\Omega_p}^2\right),$$

where $\kappa_1=\frac{2gC_1}{\sqrt{\nu S_0k_{\min}}}$. Combining the initial condition given in (23) with the definition of P_h in (21), we get $\|\underline{\boldsymbol{w}}_{1,h}^0\|_0=\|P_h^w\underline{\boldsymbol{w}}^0\|_0\leq\|\underline{\boldsymbol{w}}^0\|_0$ and $\|\underline{\boldsymbol{w}}_{1,h}^0\|_W=\|P_h^w\underline{\boldsymbol{w}}^0\|_W\leq\|\underline{\boldsymbol{w}}^0\|_W$. It is easy to conclude the result of stability (33). □

To simplify the later analysis, let us rewrite Algorithm 3.1 in the following compact form from the definition of numerical solutions in (26): find $\left(\underline{\boldsymbol{w}}_{2,h}^{n+1},p_{2,h}^{n+1}\right)\in\boldsymbol{W}_h\times Q_h$ such that $\forall\left(\underline{\boldsymbol{z}}_h,q_h\right)\in\boldsymbol{W}_h\times Q_h$,

$$\begin{cases}\left[\dfrac{\underline{\boldsymbol{w}}_{2,h}^{n+1}-\underline{\boldsymbol{w}}_{2,h}^n}{\Delta t},\underline{\boldsymbol{z}}_h\right]+a\left(\underline{\boldsymbol{w}}_{2,h}^{n+1},\underline{\boldsymbol{z}}_h\right)+b\left(\underline{\boldsymbol{z}}_h,p_{2,h}^{n+1}\right)\\ \quad=-a_\Gamma\left(\underline{\boldsymbol{w}}_{2,h}^n,\underline{\boldsymbol{z}}_h\right)+a\left(\dfrac{\underline{\boldsymbol{w}}_{1,h}^{n+1}-\underline{\boldsymbol{w}}_{1,h}^n}{2},\underline{\boldsymbol{z}}_h\right)-a_\Gamma\left(\dfrac{\underline{\boldsymbol{w}}_{1,h}^{n+1}-\underline{\boldsymbol{w}}_{1,h}^n}{2},\underline{\boldsymbol{z}}_h\right)+b\left(\underline{\boldsymbol{z}}_h,\dfrac{p_{1,h}^{n+1}-p_{1,h}^n}{2}\right)+\left(\dfrac{\boldsymbol{f}^{n+1}+\boldsymbol{f}^n}{2},\underline{\boldsymbol{z}}_h\right),\\ b\left(\underline{\boldsymbol{w}}_{2,h}^{n+1},q_h\right)=0,\\ \underline{\boldsymbol{w}}_{2,h}^0=P_h^w\underline{\boldsymbol{w}}^0.\end{cases} \tag{39}$$

Theorem 4.1. *Under the assumption (32), we have the following stability result*

$$\|\underline{\boldsymbol{w}}_{2,h}^m\|_0^2+\Delta t\sum_{n=0}^{m}\|\underline{\boldsymbol{w}}_{2,h}^{n}\|_W^2\leq C\left(d,\alpha,\nu,g,S_0,k_{min},T\right)\left(\|\underline{\boldsymbol{w}}^0\|_0+\Delta t\|\underline{\boldsymbol{w}}^0\|_W^2+\Delta t\sum_{n=0}^{m}\|\boldsymbol{f}_1^n\|_{\Omega_f}^2+g\Delta t\sum_{n=0}^{m}\|f_2^n\|_{\Omega_p}^2\right). \tag{40}$$

Here $C\left(d,\alpha,\nu,g,S_0,k_{min},T\right)$ denotes a generic positive constant only depending on the data $\left(d,\alpha,\nu,g,S_0,k_{min},T\right)$.

Proof. Taking $\underline{\boldsymbol{z}}_h=2\Delta t\underline{\boldsymbol{w}}_{2,h}^{n+1}$ in (39), we have

$$\|\underline{\boldsymbol{w}}_{2,h}^{n+1}\|_0^2-\|\underline{\boldsymbol{w}}_{2,h}^n\|_0^2+\|\underline{\boldsymbol{w}}_{2,h}^{n+1}-\underline{\boldsymbol{w}}_{2,h}^n\|_0^2+2\Delta t\|\underline{\boldsymbol{w}}_{2,h}^{n+1}\|_W^2+2\Delta t\sum_{i=1}^{d-1}\frac{\alpha\sqrt{\nu g}}{\sqrt{\mathrm{tr}(\boldsymbol{K})}}\|\underline{\boldsymbol{w}}_{2,h}^{n+1}\cdot\tau_i\|_{L^2(\Gamma)}^2$$
$$=\Delta ta\left(\underline{\boldsymbol{w}}_{1,h}^{n+1}-\underline{\boldsymbol{w}}_{1,h}^n,\underline{\boldsymbol{w}}_{2,h}^{n+1}\right)-2\Delta ta_\Gamma\left(\underline{\boldsymbol{w}}_{2,h}^n,\underline{\boldsymbol{w}}_{2,h}^{n+1}\right)-\Delta ta_\Gamma\left(\underline{\boldsymbol{w}}_{1,h}^{n+1}-\underline{\boldsymbol{w}}_{1,h}^n,\underline{\boldsymbol{w}}_{2,h}^{n+1}\right)+\Delta t\left(\boldsymbol{f}^{n+1}+\boldsymbol{f}^n,\underline{\boldsymbol{w}}_{2,h}^{n+1}\right). \tag{41}$$

For the bilinear term on the right hand side of (41), we have

$$\Delta ta(\underline{\boldsymbol{w}}_{1,h}^{n+1}-\underline{\boldsymbol{w}}_{1,h}^n,\underline{\boldsymbol{w}}_{2,h}^{n+1})=\Delta ta_f(\boldsymbol{u}_{1,h}^{n+1}-\boldsymbol{u}_{1,h}^n,\boldsymbol{u}_{2,h}^{n+1})+\Delta ta_p(\varphi_{1,h}^{n+1}-\varphi_{1,h}^n,\varphi_{2,h}^{n+1}). \tag{42}$$

Using the Hölder, trace, Poincaré and Young's inequalities, we can obtain

$$
\begin{aligned}
&\Delta t a_f(\boldsymbol{u}_{1,h}^{n+1}-\boldsymbol{u}_{1,h}^{n},\boldsymbol{u}_{2,h}^{n+1}) = \nu\Delta t\left(\nabla(\boldsymbol{u}_{1,h}^{n+1}-\boldsymbol{u}_{1,h}^{n}),\nabla\boldsymbol{u}_{2,h}^{n+1}\right)_{\Omega_f} + \Delta t\sum_{i=1}^{d-1}\int_{\Gamma}\frac{\alpha\sqrt{\nu g}}{\sqrt{\mathrm{tr}(\boldsymbol{K})}}\left((\boldsymbol{u}_{1,h}^{n+1}-\boldsymbol{u}_{1,h}^{n})\cdot\boldsymbol{\tau}_i\right)\left(\boldsymbol{u}_{2,h}^{n+1}\cdot\boldsymbol{\tau}_i\right)\\
&\le \nu\Delta t\|\nabla(\boldsymbol{u}_{1,h}^{n+1}-\boldsymbol{u}_{1,h}^{n})\|_{\Omega_f}\|\nabla\boldsymbol{u}_{2,h}^{n+1}\|_{\Omega_f} + \Delta t C_t C_p^{\frac{1}{2}}\sum_{i=1}^{d-1}\frac{\alpha\sqrt{\nu g}}{\sqrt{\mathrm{tr}(\boldsymbol{K})}}\|\nabla(\boldsymbol{u}_{1,h}^{n+1}-\boldsymbol{u}_{1,h}^{n})\|_{\Omega_f}\|\boldsymbol{u}_{2,h}^{n+1}\cdot\boldsymbol{\tau}_i\|_{L^2(\Gamma)}\\
&\le \varepsilon\nu\Delta t\|\nabla\boldsymbol{u}_{2,h}^{n+1}\|_{\Omega_f}^2 + \frac{\nu}{4\varepsilon}\Delta t\|\nabla(\boldsymbol{u}_{1,h}^{n+1}-\boldsymbol{u}_{1,h}^{n})\|_{\Omega_f}^2 + \varepsilon\Delta t\sum_{i=1}^{d-1}\frac{\alpha\sqrt{\nu g}}{\sqrt{\mathrm{tr}(\boldsymbol{K})}}\|\boldsymbol{u}_{2,h}^{n+1}\cdot\tau_i\|_{L^2(\Gamma)}^2\\
&\quad + \frac{C_t^2C_p}{4\varepsilon}\Delta t\sum_{i=1}^{d-1}\frac{\alpha\sqrt{\nu g}}{\sqrt{\mathrm{tr}(\boldsymbol{K})}}\|\nabla(\boldsymbol{u}_{1,h}^{n+1}-\boldsymbol{u}_{1,h}^{n})\|_{\Omega_f}^2\\
&\le \varepsilon\nu\Delta t\|\nabla\boldsymbol{u}_{2,h}^{n+1}\|_{\Omega_f}^2 + \varepsilon\Delta t\sum_{i=1}^{d-1}\frac{\alpha\sqrt{\nu g}}{\sqrt{\mathrm{tr}(\boldsymbol{K})}}\|\boldsymbol{u}_{2,h}^{n+1}\cdot\tau_i\|_{L^2(\Gamma)}^2 + \left(\frac{1}{4\varepsilon}+\frac{C_t^2C_p(d-1)\alpha g}{4\varepsilon\sqrt{\nu g k_{\min}}}\right)\nu\Delta t\|\nabla(\boldsymbol{u}_{1,h}^{n+1}-\boldsymbol{u}_{1,h}^{n})\|_{\Omega_f}^2,
\end{aligned}
\tag{43}
$$

and

$$
\begin{aligned}
\Delta t a_p(\varphi_{1,h}^{n+1}-\varphi_{1,h}^{n},\varphi_{2,h}^{n+1}) &= g\Delta t\left(\boldsymbol{K}\nabla(\varphi_{1,h}^{n+1}-\varphi_{1,h}^{n}),\nabla\varphi_{2,h}^{n+1}\right)_{\Omega_p}\\
&\le g\Delta t\|\boldsymbol{K}^{\frac{1}{2}}\nabla(\varphi_{1,h}^{n+1}-\varphi_{1,h}^{n})\|_{\Omega_p}\|\boldsymbol{K}^{\frac{1}{2}}\nabla\varphi_{2,h}^{n+1}\|_{\Omega_p}\\
&\le \varepsilon g\Delta t\|\boldsymbol{K}^{\frac{1}{2}}\nabla\varphi_{2,h}^{n+1}\|_{\Omega_p}^2 + \frac{1}{4\varepsilon}g\Delta t\|\boldsymbol{K}^{\frac{1}{2}}\nabla(\varphi_{1,h}^{n+1}-\varphi_{1,h}^{n})\|_{\Omega_p}^2.
\end{aligned}
$$

Then considering the definition of norms in (14), and combining the above two estimates with (42) lead to

$$
\Delta t a(\underline{\boldsymbol{w}}_{1,h}^{n+1}-\underline{\boldsymbol{w}}_{1,h}^{n},\underline{\boldsymbol{w}}_{2,h}^{n+1}) \le \varepsilon\Delta t\|\underline{\boldsymbol{w}}_{2,h}^{n+1}\|_W^2 + \varepsilon\Delta t\sum_{i=1}^{d-1}\frac{\alpha\sqrt{\nu g}}{\sqrt{\mathrm{tr}(\boldsymbol{K})}}\|\boldsymbol{u}_{2,h}^{n+1}\cdot\tau_i\|_{L^2(\Gamma)}^2 + \left(\frac{1}{4\varepsilon}+\frac{C_t^2C_p(d-1)\alpha g}{4\varepsilon\sqrt{\nu g k_{\min}}}\right)\Delta t\|\underline{\boldsymbol{w}}_{1,h}^{n+1}-\underline{\boldsymbol{w}}_{1,h}^{n}\|_W^2. \tag{44}
$$

Next, we bound the interface terms on the right hand side of (41). From (16) and (30), we get

$$
\begin{aligned}
&-2\Delta t a_\Gamma(\underline{\boldsymbol{w}}_{2,h}^{n},\underline{\boldsymbol{w}}_{2,h}^{n+1}) = 2\Delta t a_\Gamma(\underline{\boldsymbol{w}}_{2,h}^{n+1},\underline{\boldsymbol{w}}_{2,h}^{n})\\
&\le \varepsilon\Delta t\left(\|\underline{\boldsymbol{w}}_{2,h}^{n+1}\|_W^2+\|\underline{\boldsymbol{w}}_{2,h}^{n}\|_W^2\right) + \frac{gC_1}{4\varepsilon\sqrt{\nu S_0 k_{\min}}}\Delta t\left(\|\underline{\boldsymbol{w}}_{2,h}^{n+1}\|_0^2+\|\underline{\boldsymbol{w}}_{2,h}^{n}\|_0^2\right).
\end{aligned}
$$

Using (16), (30) and the Poincaré inequality leads to

$$
\begin{aligned}
&-\Delta t a_\Gamma(\underline{\boldsymbol{w}}_{1,h}^{n+1}-\underline{\boldsymbol{w}}_{1,h}^{n},\underline{\boldsymbol{w}}_{2,h}^{n+1}) = \Delta t a_\Gamma(\underline{\boldsymbol{w}}_{2,h}^{n+1},\underline{\boldsymbol{w}}_{1,h}^{n+1}-\underline{\boldsymbol{w}}_{1,h}^{n})\\
&\le \varepsilon\Delta t\left(\|\underline{\boldsymbol{w}}_{2,h}^{n+1}\|_W^2+\|\underline{\boldsymbol{w}}_{1,h}^{n+1}-\underline{\boldsymbol{w}}_{1,h}^{n}\|_W^2\right) + \frac{gC_1}{8\varepsilon\sqrt{\nu S_0 k_{\min}}}\Delta t\left(\|\underline{\boldsymbol{w}}_{2,h}^{n+1}\|_0^2+\|\underline{\boldsymbol{w}}_{1,h}^{n+1}-\underline{\boldsymbol{w}}_{1,h}^{n}\|_0^2\right)\\
&\le \varepsilon\Delta t\|\underline{\boldsymbol{w}}_{2,h}^{n+1}\|_W^2 + \frac{gC_1}{8\varepsilon\sqrt{\nu S_0 k_{\min}}}\Delta t\|\underline{\boldsymbol{w}}_{2,h}^{n+1}\|_0^2 + \left(\varepsilon+\frac{gC_1(C_p^2+\tilde{C}_p^2)}{8\varepsilon\sqrt{\nu S_0 k_{\min}}}\right)\Delta t\|\underline{\boldsymbol{w}}_{1,h}^{n+1}-\underline{\boldsymbol{w}}_{1,h}^{n}\|_W^2.
\end{aligned}
$$

In a similar way of (36), we obtain

$$
\Delta t(\boldsymbol{f}^{n+1}+\boldsymbol{f}^{n},\underline{\boldsymbol{w}}_{2,h}^{n+1}) \le \varepsilon\Delta t\|\underline{\boldsymbol{w}}_{2,h}^{n+1}\|_W^2 + \frac{C_p^2}{4\varepsilon\nu}\Delta t\|\boldsymbol{f}_1^{n+1}+\boldsymbol{f}_1^{n}\|_{\Omega_f}^2 + \frac{g\tilde{C}_p^2}{4\varepsilon k_{\min}}\Delta t\|f_2^{n+1}+f_2^{n}\|_{\Omega_p}^2.
$$

Combining the above estimates with (41), setting $\varepsilon = 1/4$ and rearranging terms result in

$$
\begin{aligned}
&\|\underline{\boldsymbol{w}}_{2,h}^{n+1}\|_0^2 - \|\underline{\boldsymbol{w}}_{2,h}^{n}\|_0^2 + \Delta t\|\underline{\boldsymbol{w}}_{2,h}^{n+1}\|_W^2 - \frac{1}{4}\Delta t\|\underline{\boldsymbol{w}}_{2,h}^{n}\|_W^2 + \Delta t\sum_{i=1}^{d-1}\frac{\alpha\sqrt{\nu g}}{\sqrt{\mathrm{tr}(\boldsymbol{K})}}\|\boldsymbol{w}_{2,h}^{n+1}\cdot\tau_i\|_{L^2(\Gamma)}^2\\
&\le \frac{3gC_1}{2\sqrt{\nu S_0 k_{\min}}}\Delta t\left(\|\underline{\boldsymbol{w}}_{2,h}^{n+1}\|_0^2+\|\underline{\boldsymbol{w}}_{2,h}^{n}\|_0^2\right) + \left(\frac{5}{4}+\frac{C_t^2C_p(d-1)\alpha g}{\sqrt{\nu g k_{\min}}}+\frac{gC_1(C_p^2+\tilde{C}_p^2)}{2\sqrt{\nu S_0 k_{\min}}}\right)\Delta t\|\underline{\boldsymbol{w}}_{1,h}^{n+1}-\underline{\boldsymbol{w}}_{1,h}^{n}\|_W\\
&\quad + \frac{C_p^2}{\nu}\Delta t\|\boldsymbol{f}_1^{n+1}+\boldsymbol{f}_1^{n}\|_{\Omega_f}^2 + \frac{g\tilde{C}_p^2}{k_{\min}}\Delta t\|f_2^{n+1}+f_2^{n}\|_{\Omega_p}^2.
\end{aligned}
\tag{45}
$$

Summing (45) over n with $0 \le n \le m-1$, and adding the term $\frac{3}{4}\Delta t\|\underline{\boldsymbol{w}}_{2,h}^{0}\|_W^2$ to both sides of the new relationship, we have

$$
\begin{aligned}
&\|\underline{\boldsymbol{w}}_{2,h}^{m}\|_0^2 + \frac{3}{4}\Delta t\sum_{n=0}^{m}\|\underline{\boldsymbol{w}}_{2,h}^{n}\|_W^2\\
&\le \|\underline{\boldsymbol{w}}_{2,h}^{0}\|_0^2 + \Delta t\|\underline{\boldsymbol{w}}_{2,h}^{0}\|_W^2 + \frac{3gC_1}{\sqrt{\nu S_0 k_{\min}}}\Delta t\sum_{n=0}^{m}\|\underline{\boldsymbol{w}}_{2,h}^{n}\|_0^2 + \left(5+\frac{4C_t^2C_p(d-1)\alpha g}{\sqrt{\nu g k_{\min}}}+\frac{2gC_1(C_p^2+\tilde{C}_p^2)}{\sqrt{\nu S_0 k_{\min}}}\right)\Delta t\sum_{n=0}^{m}\|\underline{\boldsymbol{w}}_{1,h}^{n}\|_W^2\\
&\quad + \frac{4C_p^2}{\nu}\Delta t\sum_{n=0}^{m}\|\boldsymbol{f}_1^{n}\|_{\Omega_f}^2 + \frac{4g\tilde{C}_p^2}{k_{\min}}\Delta t\sum_{n=0}^{m}\|f_2^{n}\|_{\Omega_p}^2.
\end{aligned}
$$

By simple calculation, we have

$$\begin{aligned}
&\|\underline{\boldsymbol{w}}_{2,h}^{m}\|_0^2+\Delta t\sum_{n=0}^{m}\|\underline{\boldsymbol{w}}_{2,h}^{n}\|_W^2\\
&\le\frac{4}{3}\|\underline{\boldsymbol{w}}_{2,h}^{0}\|_0^2+\frac{4}{3}\Delta t\|\underline{\boldsymbol{w}}_{2,h}^{0}\|_W^2+\frac{4gC_1}{\sqrt{\nu S_0 k_{\min}}}\Delta t\sum_{n=0}^{m}\|\underline{\boldsymbol{w}}_{2,h}^{n}\|_0^2+\left(\frac{20}{3}+\frac{16C_t^2C_p(d-1)\alpha g}{3\sqrt{\nu g k_{\min}}}+\frac{8gC_1(C_p^2+\tilde{C}_p^2)}{3\sqrt{\nu S_0 k_{\min}}}\right)\Delta t\sum_{n=0}^{m}\|\underline{\boldsymbol{w}}_{1,h}^{n}\|_W^2\\
&\quad+\frac{16C_p^2}{3\nu}\Delta t\sum_{n=0}^{m}\|\boldsymbol{f}_1^n\|_{\Omega_f}^2+\frac{16g\tilde{C}_p^2}{3k_{\min}}\Delta t\sum_{n=0}^{m}\|f_2^n\|_{\Omega_p}^2.
\end{aligned}$$

By taking into account the condition (32) and applying the Gronwall inequality, we acquire

$$\begin{aligned}
&\|\underline{\boldsymbol{w}}_{2,h}^{m}\|_0^2+\Delta t\sum_{n=1}^{m}\|\underline{\boldsymbol{w}}_{2,h}^{n}\|_W^2\\
&\le\exp\left(\Delta t\sum_{n=0}^{m}\frac{\kappa_2}{1-\Delta t\kappa_2}\right)\left\{\frac{4}{3}\|\underline{\boldsymbol{w}}_{2,h}^{0}\|_0^2+\frac{4}{3}\Delta t\|\underline{\boldsymbol{w}}_{2,h}^{0}\|_W^2+\left(\frac{20}{3}+\frac{16C_t^2C_p(d-1)\alpha g}{3\sqrt{\nu g k_{\min}}}+\frac{8gC_1(C_p^2+\tilde{C}_p^2)}{3\sqrt{\nu S_0 k_{\min}}}\right)\Delta t\sum_{n=0}^{m}\|\underline{\boldsymbol{w}}_{1,h}^{n}\|_W^2\right.\\
&\quad\left.+\frac{16C_p^2}{3\nu}\Delta t\sum_{n=0}^{m}\|\boldsymbol{f}_1^n\|_{\Omega_f}^2+\frac{16g\tilde{C}_p^2}{3k_{\min}}\Delta t\sum_{n=0}^{m}\|f_2^n\|_{\Omega_p}^2\right\},
\end{aligned}\tag{46}$$

where $\kappa_2=\frac{4gC_1}{\sqrt{\nu S_0 k_{\min}}}$. Thanks to the estimate (33), and the relations $\|\underline{\boldsymbol{w}}_{2,h}^{0}\|_0=\|P_h^w\underline{\boldsymbol{w}}^0\|_0\le\|\underline{\boldsymbol{w}}^0\|_0$ and $\|\underline{\boldsymbol{w}}_{2,h}^{0}\|_W=\|P_h^w\underline{\boldsymbol{w}}^0\|_W\le\|\underline{\boldsymbol{w}}^0\|_W$, we complete the proof of this theorem. □

5. Convergence analysis

In this section, we study the errors of Algorithm 3.1. Define $\left(\underline{\boldsymbol{w}}^m,p^m\right)=\left(\underline{\boldsymbol{w}}(t^m),p(t^m)\right)$ and $\left(\tilde{\underline{\boldsymbol{w}}}^m,\tilde{p}^m\right)=\left(P_h^w\underline{\boldsymbol{w}}^m,P_h^p p^m\right)$. Then, let us denote: $i=1,2$,

$$\begin{aligned}
&\left(\underline{\boldsymbol{w}}_{i,h}^m-\tilde{\underline{\boldsymbol{w}}}^m\right)-\left(\underline{\boldsymbol{w}}^m-\tilde{\underline{\boldsymbol{w}}}^m\right)=\underline{\boldsymbol{e}}_{i,h}^m-\underline{\boldsymbol{\xi}}^m,\\
&\left(p_{i,h}^m-\tilde{p}^m\right)-\left(p^m-\tilde{p}^m\right)=\epsilon_{i,h}^m-\eta^m.
\end{aligned}\tag{47}$$

Here, $\underline{\boldsymbol{e}}_{i,h}^m=(\boldsymbol{e}_{i,f}^m,e_{i,p}^m)$ and $\underline{\boldsymbol{\xi}}^m=(\boldsymbol{\xi}_f^m,\xi_p^m)$. In particular, $\underline{\boldsymbol{e}}_{i,h}^0=(\mathbf{0},0)$.

The error estimate of the first-order decoupled scheme (23) has been provided in the previous literature [21]. However, we provide the error estimation results in Lemma 5.1 with the different regularity conditions (48) and the time step restriction (49). The rigorous proof is akin to the process in [22,25], but simpler, so we skip it here.

Lemma 5.1. *Assume the exact solution of Stokes/Darcy model satisfies*

$$\boldsymbol{u}_t\in L^2\left(0,T;H^{k_1+1}(\Omega_f)^d\right),\ \boldsymbol{u}_{tt}\in L^2\left(0,T;L^2(\Omega_f)^d\right),\ \varphi_t\in L^2\left(0,T;H^{k_2+1}(\Omega_p)\right),\ \varphi_{tt}\in L^2\left(0,T;L^2(\Omega_p)\right).\tag{48}$$

Under the condition

$$\frac{5gC_1}{h}\max\left\{\frac{\tilde{C}_pC_I}{k_{\min}},\frac{C_p\tilde{C}_I}{\nu S_0}\right\}\Delta t<1,\tag{49}$$

we have,

$$\|\underline{\boldsymbol{e}}_{1,h}^m\|_0^2+\Delta t\sum_{n=0}^{m-1}\|\underline{\boldsymbol{e}}_{1,h}^{n+1}\|_W^2\le C(\nu,g,S_0,k_{\min})\left(\Delta t^2+h^{2k_1+2}+h^{2k_2+2}\right).\tag{50}$$

Next, we provide the bounds of $d_t\underline{\boldsymbol{e}}_{1,h}^m=\frac{\underline{\boldsymbol{e}}_{1,h}^m-\underline{\boldsymbol{e}}_{1,h}^{m-1}}{\Delta t}$ in Lemma 5.2.

Lemma 5.2. *Under the assumptions in Lemma 5.1 and the regularities*

$$\boldsymbol{u}_{tt}\in L^2\left(0,T;H^{k_1}(\Omega_f)^d\right),\ \boldsymbol{u}_{ttt}\in L^2\left(0,T;L^2(\Omega_f)^d\right),\ \varphi_{tt}\in L^2\left(0,T;H^{k_2}(\Omega_p)\right),\ \varphi_{ttt}\in L^2\left(0,T;L^2(\Omega_p)\right),\tag{51}$$

we have,

$$\|d_t\underline{\boldsymbol{e}}_{1,h}^m\|_0^2+\Delta t\sum_{n=0}^{m-1}\|d_t\underline{\boldsymbol{e}}_{1,h}^{n+1}\|_W^2\le C(\nu,g,S_0,k_{\min})\left(\Delta t^2+h^{2k_1}+h^{2k_2}+\frac{\Delta t^2}{h}\right).\tag{52}$$

Proof. At time t^{n+1}, we can deduce the following equations from (15):

$$\begin{cases} \left[\dfrac{\underline{\boldsymbol{w}}^{n+1}-\underline{\boldsymbol{w}}^{n}}{\Delta t},\underline{\boldsymbol{z}}\right]+a\left(\underline{\boldsymbol{w}}^{n+1},\underline{\boldsymbol{z}}\right)+a_{\Gamma}\left(\underline{\boldsymbol{w}}^{n+1},\underline{\boldsymbol{z}}\right)+b\left(\underline{\boldsymbol{z}},p^{n+1}\right)=\left[\dfrac{\underline{\boldsymbol{w}}^{n+1}-\underline{\boldsymbol{w}}^{n}}{\Delta t}-\underline{\boldsymbol{w}}_t^{n+1},\underline{\boldsymbol{z}}\right]+\left(\boldsymbol{f}^{n+1},\underline{\boldsymbol{z}}\right), \quad \forall \underline{\boldsymbol{z}}\in \boldsymbol{W}, \\ b\left(\underline{\boldsymbol{w}}^{n+1},q\right)=0, \quad \forall q\in Q. \end{cases} \tag{53}$$

From the definition of P_h in (21), we can get

$$a\left(\underline{\xi}^{n+1},\underline{\boldsymbol{z}}_h\right)+b\left(\underline{\boldsymbol{z}}_h,\eta^{n+1}\right)=-a_{\Gamma}\left(\underline{\xi}^{n+1},\underline{\boldsymbol{z}}_h\right), \quad \forall \underline{\boldsymbol{z}}_h\in \boldsymbol{W}_h. \tag{54}$$

Let $(\underline{\boldsymbol{z}},q)=(\boldsymbol{v}_h,q_h)$ in (53) and subtract it from (23). Considering (47) and (54), we derive the following error equations: $\forall \underline{\boldsymbol{z}}_h\in \boldsymbol{W}_h$ and $q_h\in Q_h$,

$$\begin{cases} \left[\dfrac{\underline{\boldsymbol{e}}_{1,h}^{n+1}-\underline{\boldsymbol{e}}_{1,h}^{n}}{\Delta t},\underline{\boldsymbol{z}}_h\right]+a\left(\underline{\boldsymbol{e}}_{1,h}^{n+1},\underline{\boldsymbol{z}}_h\right)+b\left(\underline{\boldsymbol{z}}_h,\epsilon_{1,h}^{n+1}\right) \\ \quad =\left[\underline{\boldsymbol{w}}_t^{n+1}-\dfrac{\underline{\boldsymbol{w}}^{n+1}-\underline{\boldsymbol{w}}^{n}}{\Delta t},\underline{\boldsymbol{z}}_h\right]+\left[\dfrac{\underline{\xi}^{n+1}-\underline{\xi}^{n}}{\Delta t},\underline{\boldsymbol{z}}_h\right]-a_{\Gamma}\left(\underline{\boldsymbol{e}}_{1,h}^{n},\underline{\boldsymbol{z}}_h\right)-\Delta t a_{\Gamma}\left(\dfrac{\underline{\xi}^{n+1}-\underline{\xi}^{n}}{\Delta t},\underline{\boldsymbol{z}}_h\right)+\Delta t a_{\Gamma}\left(\dfrac{\underline{\boldsymbol{w}}^{n+1}-\underline{\boldsymbol{w}}^{n}}{\Delta t},\underline{\boldsymbol{z}}_h\right), \\ b\left(\underline{\boldsymbol{e}}_{1,h}^{n+1},q_h\right)=0. \end{cases} \tag{55}$$

Considering (55) at time t^n and subtracting the new equations from (55) yield

$$\begin{cases} \left[d_t\underline{\boldsymbol{e}}_{1,h}^{n+1}-d_t\underline{\boldsymbol{e}}_{1,h}^{n},\underline{\boldsymbol{z}}_h\right]+\Delta t a\left(d_t\underline{\boldsymbol{e}}_{1,h}^{n+1},\underline{\boldsymbol{z}}_h\right)+\Delta t b\left(\underline{\boldsymbol{z}}_h,d_t\epsilon_{1,h}^{n+1}\right) \\ \quad =\left[\underline{\boldsymbol{w}}_t^{n+1}-\dfrac{\underline{\boldsymbol{w}}^{n+1}-\underline{\boldsymbol{w}}^{n}}{\Delta t}-\underline{\boldsymbol{w}}_t^{n}+\dfrac{\underline{\boldsymbol{w}}^{n}-\underline{\boldsymbol{w}}^{n-1}}{\Delta t},\underline{\boldsymbol{z}}_h\right]+\left[\dfrac{\underline{\xi}^{n+1}-\underline{\xi}^{n}}{\Delta t}-\dfrac{\underline{\xi}^{n}-\underline{\xi}^{n-1}}{\Delta t},\underline{\boldsymbol{z}}_h\right] \\ \quad -\Delta t a_{\Gamma}\left(d_t\underline{\boldsymbol{e}}_{1,h}^{n},\underline{\boldsymbol{z}}_h\right)-\Delta t a_{\Gamma}\left(\dfrac{\underline{\xi}^{n+1}-\underline{\xi}^{n}}{\Delta t}-\dfrac{\underline{\xi}^{n}-\underline{\xi}^{n-1}}{\Delta t},\underline{\boldsymbol{z}}_h\right)+\Delta t a_{\Gamma}\left(\dfrac{\underline{\boldsymbol{w}}^{n+1}-\underline{\boldsymbol{w}}^{n}}{\Delta t}-\dfrac{\underline{\boldsymbol{w}}^{n}-\underline{\boldsymbol{w}}^{n-1}}{\Delta t},\underline{\boldsymbol{z}}_h\right), \\ b\left(d_t\underline{\boldsymbol{e}}_{1,h}^{n+1},q_h\right)=0, \end{cases}$$

where $d_t\underline{\boldsymbol{e}}_{1,h}^{n+1}=\frac{\underline{\boldsymbol{e}}_{1,h}^{n+1}-\underline{\boldsymbol{e}}_{1,h}^{n}}{\Delta t}$ and $d_t\epsilon_{1,h}^{n+1}=\frac{\epsilon_{1,h}^{n+1}-\epsilon_{1,h}^{n}}{\Delta t}$. Taking $\underline{\boldsymbol{z}}_h=2d_t\underline{\boldsymbol{e}}_{1,h}^{n+1}$ and $q_h=d_t\epsilon_{1,h}^{n+1}$ in the above equations, we have

$$\begin{aligned} &\left\|d_t\underline{\boldsymbol{e}}_{1,h}^{n+1}\right\|_0^2-\left\|d_t\underline{\boldsymbol{e}}_{1,h}^{n}\right\|_0^2+\left\|d_t\underline{\boldsymbol{e}}_{1,h}^{n+1}-d_t\underline{\boldsymbol{e}}_{1,h}^{n}\right\|_0^2+2\Delta t\left\|d_t\underline{\boldsymbol{e}}_{1,h}^{n+1}\right\|_W^2 \\ &\le 2\left[\underline{\boldsymbol{w}}_t^{n+1}-\dfrac{\underline{\boldsymbol{w}}^{n+1}-\underline{\boldsymbol{w}}^{n}}{\Delta t}-\underline{\boldsymbol{w}}_t^{n}+\dfrac{\underline{\boldsymbol{w}}^{n}-\underline{\boldsymbol{w}}^{n-1}}{\Delta t},d_t\underline{\boldsymbol{e}}_{1,h}^{n+1}\right]+2\left[\dfrac{\underline{\xi}^{n+1}-\underline{\xi}^{n}}{\Delta t}-\dfrac{\underline{\xi}^{n}-\underline{\xi}^{n-1}}{\Delta t},d_t\underline{\boldsymbol{e}}_{1,h}^{n+1}\right] \\ &\quad -2\Delta t a_{\Gamma}\left(d_t\underline{\boldsymbol{e}}_{1,h}^{n},d_t\underline{\boldsymbol{e}}_{1,h}^{n+1}\right)-2\Delta t a_{\Gamma}\left(\dfrac{\underline{\xi}^{n+1}-\underline{\xi}^{n}}{\Delta t}-\dfrac{\underline{\xi}^{n}-\underline{\xi}^{n-1}}{\Delta t},d_t\underline{\boldsymbol{e}}_{1,h}^{n+1}\right)+2\Delta t a_{\Gamma}\left(\dfrac{\underline{\boldsymbol{w}}^{n+1}-\underline{\boldsymbol{w}}^{n}}{\Delta t}-\dfrac{\underline{\boldsymbol{w}}^{n}-\underline{\boldsymbol{w}}^{n-1}}{\Delta t},d_t\underline{\boldsymbol{e}}_{1,h}^{n+1}\right). \end{aligned} \tag{56}$$

Utilizing the Hölder, Poincaré and Young's inequalities and (18), we obtain, $\forall \varepsilon_1>0$,

$$\begin{aligned} &2\left(\boldsymbol{u}_t^{n+1}-\dfrac{\boldsymbol{u}^{n+1}-\boldsymbol{u}^{n}}{\Delta t}-\boldsymbol{u}_t^{n}+\dfrac{\boldsymbol{u}^{n}-\boldsymbol{u}^{n-1}}{\Delta t},d_t\boldsymbol{e}_{1,f}^{n+1}\right)_{\Omega_f}+2\left(\dfrac{\xi_f^{n+1}-\xi_f^{n}}{\Delta t}-\dfrac{\xi_f^{n}-\xi_f^{n-1}}{\Delta t},d_t\boldsymbol{e}_{1,f}^{n+1}\right)_{\Omega_f} \\ &\le 2\varepsilon_1\nu\Delta t\|\nabla d_t\boldsymbol{e}_{1,f}^{n+1}\|_{\Omega_f}^2+\dfrac{C_p^2}{\varepsilon_1\nu\Delta t}\left(\left\|\boldsymbol{u}_t^{n+1}-\dfrac{\boldsymbol{u}^{n+1}-\boldsymbol{u}^{n}}{\Delta t}-\boldsymbol{u}_t^{n}+\dfrac{\boldsymbol{u}^{n}-\boldsymbol{u}^{n-1}}{\Delta t}\right\|_{\Omega_f}^2+\left\|\dfrac{\xi_f^{n+1}-\xi_f^{n}}{\Delta t}-\dfrac{\xi_f^{n}-\xi_f^{n-1}}{\Delta t}\right\|_{\Omega_f}^2\right). \end{aligned} \tag{57}$$

Using the Minkowski inequality and the relation

$$(a+b+c)^2\le 3a^2+3b^2+3c^2, \quad \forall a,b,c\in \mathbb{R}^d,$$

we get

$$
\begin{aligned}
&\left\|\boldsymbol{u}_t^{n+1}-\frac{\boldsymbol{u}^{n+1}-\boldsymbol{u}^n}{\Delta t}-\boldsymbol{u}_t^n+\frac{\boldsymbol{u}^n-\boldsymbol{u}^{n-1}}{\Delta t}\right\|_{\Omega_f}^2\\
&=\left\|\left(\frac{\boldsymbol{u}_t^{n+1}+\boldsymbol{u}_t^n}{2}-\frac{\boldsymbol{u}^{n+1}-\boldsymbol{u}^n}{\Delta t}\right)-\left(\frac{\boldsymbol{u}_t^n+\boldsymbol{u}_t^{n-1}}{2}-\frac{\boldsymbol{u}^n-\boldsymbol{u}^{n-1}}{\Delta t}\right)+\frac{\boldsymbol{u}_t^{n+1}-2\boldsymbol{u}_t^n+\boldsymbol{u}_t^{n-1}}{2}\right\|_{\Omega_f}^2\\
&\le\left(\left\|\frac{\boldsymbol{u}_t^{n+1}+\boldsymbol{u}_t^n}{2}-\frac{\boldsymbol{u}^{n+1}-\boldsymbol{u}^n}{\Delta t}\right\|_{\Omega_f}+\left\|\frac{\boldsymbol{u}_t^n+\boldsymbol{u}_t^{n-1}}{2}-\frac{\boldsymbol{u}^n-\boldsymbol{u}^{n-1}}{\Delta t}\right\|_{\Omega_f}+\left\|\frac{\boldsymbol{u}_t^{n+1}-2\boldsymbol{u}_t^n+\boldsymbol{u}_t^{n-1}}{2}\right\|_{\Omega_f}\right)^2\\
&\le 3\left\|\frac{\boldsymbol{u}_t^{n+1}+\boldsymbol{u}_t^n}{2}-\frac{\boldsymbol{u}^{n+1}-\boldsymbol{u}^n}{\Delta t}\right\|_{\Omega_f}^2+3\left\|\frac{\boldsymbol{u}_t^n+\boldsymbol{u}_t^{n-1}}{2}-\frac{\boldsymbol{u}^n-\boldsymbol{u}^{n-1}}{\Delta t}\right\|_{\Omega_f}^2+\frac{3}{4}\left\|\boldsymbol{u}_t^{n+1}-2\boldsymbol{u}_t^n+\boldsymbol{u}_t^{n-1}\right\|_{\Omega_f}^2.
\end{aligned}
$$

From the Hölder inequality, we get

$$
\begin{aligned}
&\left\|\frac{\boldsymbol{u}_t^{n+1}+\boldsymbol{u}_t^n}{2}-\frac{\boldsymbol{u}^{n+1}-\boldsymbol{u}^n}{\Delta t}\right\|_{\Omega_f}^2=\left\|\frac{\boldsymbol{u}_t^{n+1}+\boldsymbol{u}_t^n}{2}-\frac{1}{\Delta t}\int_{t^n}^{t^{n+1}}\boldsymbol{u}_t dt\right\|_{\Omega_f}^2\\
&\le\left\|\frac{1}{2\Delta t}\int_{t^n}^{t^{n+1}}(t-t^n)(t-t^{n+1})\boldsymbol{u}_{ttt}dt\right\|_{\Omega_f}^2\\
&\le\frac{1}{\Delta t^2}\left(\int_{t^n}^{t^{n+1}}(t-t^n)^2(t-t^{n+1})^2dt\right)\left(\int_{t^n}^{t^{n+1}}\|\boldsymbol{u}_{ttt}\|_{\Omega_f}^2\,dt\right)\\
&\le C\Delta t^3\int_{t^n}^{t^{n+1}}\|\boldsymbol{u}_{ttt}\|_{\Omega_f}^2\,dt.
\end{aligned}
$$

From the Hölder and Minkowski inequalities, we have

$$
\begin{aligned}
\left\|\boldsymbol{u}_t^{n+1}-2\boldsymbol{u}_t^n+\boldsymbol{u}_t^{n-1}\right\|_{\Omega_f}^2&\le\left\|\int_{t^n}^{t^{n+1}}(t^{n+1}-t)\boldsymbol{u}_{ttt}dt\right\|_{\Omega_f}^2+\left\|\int_{t^{n-1}}^{t^n}(t-t^{n-1})\boldsymbol{u}_{ttt}dt\right\|_{\Omega_f}^2\\
&\le\left(\int_{t^n}^{t^{n+1}}(t^{n+1}-t)^2dt\right)\left(\int_{t^n}^{t^{n+1}}\|\boldsymbol{u}_{ttt}\|_{\Omega_f}^2\,dt\right)+\left(\int_{t^{n-1}}^{t^n}(t-t^{n-1})^2dt\right)\left(\int_{t^{n-1}}^{t^n}\|\boldsymbol{u}_{ttt}\|_{\Omega_f}^2\,dt\right)\\
&\le C\Delta t^3\int_{t^{n-1}}^{t^{n+1}}\|\boldsymbol{u}_{ttt}\|_{\Omega_f}^2\,dt.
\end{aligned}
$$

Hence, we obtain

$$
\left\|\boldsymbol{u}_t^{n+1}-\frac{\boldsymbol{u}^{n+1}-\boldsymbol{u}^n}{\Delta t}-\boldsymbol{u}_t^n+\frac{\boldsymbol{u}^n-\boldsymbol{u}^{n-1}}{\Delta t}\right\|_{\Omega_f}^2\le C\Delta t^3\int_{t^{n-1}}^{t^{n+1}}\|\boldsymbol{u}_{ttt}\|_{\Omega_f}^2\,dt.
$$

For the last term on the right hand side of (57), using the Hölder and Minkowski inequalities, we get

$$
\begin{aligned}
\left\|\frac{\xi_f^{n+1}-\xi_f^n}{\Delta t}-\frac{\xi_f^n-\xi_f^{n-1}}{\Delta t}\right\|_{\Omega_f}^2&\le 2\left\|\frac{\xi_f^{n+1}-\xi_f^n}{\Delta t}-(\xi_f)_t^n\right\|_{\Omega_f}^2+2\left\|(\xi_f)_t^n-\frac{\xi_f^n-\xi_f^{n-1}}{\Delta t}\right\|_{\Omega_f}^2\\
&=2\left\|\frac{1}{\Delta t}\int_{t^n}^{t^{n+1}}(t^{n+1}-t)(\xi_f)_{tt}dt\right\|_{\Omega_f}^2+2\left\|\frac{1}{\Delta t}\int_{t^{n-1}}^{t^n}(t-t^{n-1})(\xi_f)_{tt}dt\right\|_{\Omega_f}^2\\
&\le\frac{2}{\Delta t^2}\left(\int_{t^n}^{t^{n+1}}(t^{n+1}-t)^2dt\right)\left(\int_{t^n}^{t^{n+1}}\left\|(\xi_f)_{tt}\right\|_{\Omega_f}^2\,dt\right)+\frac{2}{\Delta t^2}\left(\int_{t^{n-1}}^{t^n}(t-t^{n-1})^2dt\right)\left(\int_{t^{n-1}}^{t^n}\left\|(\xi_f)_{tt}\right\|_{\Omega_f}^2\,dt\right)
\end{aligned}
$$

$$\leq C\Delta t \int_{t^{n-1}}^{t^{n+1}} \left\|(\xi_f)_{tt}\right\|^2_{\Omega_f} dt.$$

So that, we obtain the estimate of (57) as follows

$$\begin{aligned}&2\left(\boldsymbol{u}_t^{n+1} - \frac{\boldsymbol{u}^{n+1}-\boldsymbol{u}^n}{\Delta t} - \boldsymbol{u}_t^n + \frac{\boldsymbol{u}^n-\boldsymbol{u}^{n-1}}{\Delta t}, d_t e_{1,f}^{n+1}\right)_{\Omega_f} + 2\left(\frac{\xi_f^{n+1}-\xi_f^n}{\Delta t} - \frac{\xi_f^n-\xi_f^{n-1}}{\Delta t}, d_t e_{1,f}^{n+1}\right)_{\Omega_f}\\
&\leq 2\varepsilon_1 \nu \Delta t \|\nabla d_t e_{1,f}^{n+1}\|^2_{\Omega_f} + \frac{CC_p^2}{\varepsilon_1 \nu}\left(\Delta t^2 \int_{t^{n-1}}^{t^{n+1}} \|\boldsymbol{u}_{ttt}\|^2_{\Omega_f} dt + \int_{t^{n-1}}^{t^{n+1}} \|(\xi_f)_{tt}\|^2_{\Omega_f} dt\right).\end{aligned}$$

Similarly, we can deduce that

$$\begin{aligned}&2gS_0\left(\varphi_t^{n+1} - \frac{\varphi^{n+1}-\varphi^n}{\Delta t} - \varphi_t^n + \frac{\varphi^n-\varphi^{n-1}}{\Delta t}, d_t e_{1,p}^{n+1}\right)_{\Omega_p} + 2gS_0\left(\frac{\xi_p^{n+1}-\xi_p^n}{\Delta t} - \frac{\xi_p^n-\xi_p^{n-1}}{\Delta t}, d_t e_{1,p}^{n+1}\right)_{\Omega_p}\\
&\leq 2\varepsilon_1 g \Delta t \|\boldsymbol{K}^{\frac{1}{2}} d_t e_{1,p}^{n+1}\|^2_{\Omega_f} + \frac{gS_0^2 C\tilde{C}_p^2}{\varepsilon_1 k_{\min}}\left(\Delta t^2 \int_{t^{n-1}}^{t^{n+1}} \|\varphi_{ttt}\|^2_{\Omega_p} dt + \int_{t^{n-1}}^{t^{n+1}} \|(\xi_p)_{tt}\|^2_{\Omega_p} dt\right).\end{aligned}$$

From the definitions in (14), the combination of the above two relations leads to

$$\begin{aligned}&2\left[\underline{\boldsymbol{w}}_t^{n+1} - \frac{\underline{\boldsymbol{w}}^{n+1}-\underline{\boldsymbol{w}}^n}{\Delta t} - \underline{\boldsymbol{w}}_t^n + \frac{\underline{\boldsymbol{w}}^n-\underline{\boldsymbol{w}}^{n-1}}{\Delta t}, d_t \underline{\boldsymbol{e}}_{1,h}^{n+1}\right] + 2\left[\frac{\underline{\xi}^{n+1}-\underline{\xi}^n}{\Delta t} - \frac{\underline{\xi}^n-\underline{\xi}^{n-1}}{\Delta t}, \underline{\boldsymbol{e}}_{1,h}^{n+1}\right]\\
&\leq 2\varepsilon_1 \Delta t \|d_t \boldsymbol{e}_{1,f}^{n+1}\|^2_W + \left(\frac{CC_p^2}{\varepsilon_1 \nu} + \frac{S_0 C\tilde{C}_p^2}{\varepsilon_1 k_{\min}}\right)\left(\Delta t^2 \int_{t^{n-1}}^{t^{n+1}} \|\underline{\boldsymbol{w}}_{ttt}\|^2_0 dt + \int_{t^{n-1}}^{t^{n+1}} \|\underline{\xi}_{tt}\|^2_0 dt\right).\end{aligned} \tag{58}$$

Using (16) and (31), we get

$$\begin{aligned}-2\Delta t a_\Gamma\left(d_t \underline{\boldsymbol{e}}_{1,h}^n, d_t \underline{\boldsymbol{e}}_{1,h}^{n+1}\right) &= 2\Delta t a_\Gamma\left(d_t \underline{\boldsymbol{e}}_{1,h}^{n+1} - d_t \underline{\boldsymbol{e}}_{1,h}^n, d_t \underline{\boldsymbol{e}}_{1,h}^{n+1}\right)\\
&\leq \varepsilon_1 \Delta t \|d_t \underline{\boldsymbol{e}}_{1,h}^{n+1}\|^2_W + \frac{gC_1}{\varepsilon_1 h}\max\left\{\frac{\tilde{C}_p C_I}{k_{\min}}, \frac{C_p \tilde{C}_I}{\nu S_0}\right\}\Delta t \|d_t \underline{\boldsymbol{e}}_{1,h}^{n+1} - d_t \underline{\boldsymbol{e}}_{1,h}^n\|^2_0.\end{aligned}$$

From (29), we bound the remaining interface terms as follows.

$$\begin{aligned}&-2\Delta t a_\Gamma\left(\frac{\underline{\xi}^{n+1}-\underline{\xi}^n}{\Delta t} - \frac{\underline{\xi}^n-\underline{\xi}^{n-1}}{\Delta t}, d_t \underline{\boldsymbol{e}}_{1,h}^{n+1}\right) + 2\Delta t a_\Gamma\left(\frac{\underline{\boldsymbol{w}}^{n+1}-\underline{\boldsymbol{w}}^n}{\Delta t} - \frac{\underline{\boldsymbol{w}}^n-\underline{\boldsymbol{w}}^{n-1}}{\Delta t}, d_t \underline{\boldsymbol{e}}_{1,h}^{n+1}\right)\\
&\leq 2\varepsilon_1 \Delta t \|d_t \underline{\boldsymbol{e}}_{1,h}^{n+1}\|^2_W + \frac{gC_1C_2}{\varepsilon_1 \nu k_{\min}}\Delta t\left(\left\|\frac{\underline{\xi}^{n+1}-\underline{\xi}^n}{\Delta t} - \frac{\underline{\xi}^n-\underline{\xi}^{n-1}}{\Delta t}\right\|^2_W + \left\|\frac{\underline{\boldsymbol{w}}^{n+1}-\underline{\boldsymbol{w}}^n}{\Delta t} - \frac{\underline{\boldsymbol{w}}^n-\underline{\boldsymbol{w}}^{n-1}}{\Delta t}\right\|^2_W\right)\\
&\leq 2\varepsilon_1 \Delta t \|d_t \underline{\boldsymbol{e}}_{1,h}^{n+1}\|^2_W + \frac{gCC_1C_2}{\varepsilon_1 \nu k_{\min}}\Delta t^2\left(\int_{t^{n-1}}^{t^{n+1}} \|\underline{\xi}_{tt}\|^2_W dt + \int_{t^{n-1}}^{t^{n+1}} \|\underline{\boldsymbol{w}}_{tt}\|^2_W dt\right).\end{aligned}$$

Combining the above bounds with (56), taking $\varepsilon_1 = 1/5$ and considering (49), straightforward computations lead to

$$\begin{aligned}&\|d_t \underline{\boldsymbol{e}}_{1,h}^{n+1}\|^2_0 - \|d_t \underline{\boldsymbol{e}}_{1,h}^n\|^2_0 + \Delta t \|d_t \underline{\boldsymbol{e}}_{1,h}^{n+1}\|^2_W\\
&\leq \left(\frac{5CC_p^2}{\nu} + \frac{5S_0 C\tilde{C}_p^2}{k_{\min}}\right)\left(\Delta t^2 \int_{t^{n-1}}^{t^{n+1}} \|\underline{\boldsymbol{w}}_{ttt}\|^2_0 dt + \int_{t^{n-1}}^{t^{n+1}} \|\underline{\xi}_{tt}\|^2_0 dt\right) + \frac{5gCC_1C_2}{\nu k_{\min}}\Delta t^2\left(\int_{t^{n-1}}^{t^{n+1}} \|\underline{\xi}_{tt}\|^2_W dt + \int_{t^{n-1}}^{t^{n+1}} \|\underline{\boldsymbol{w}}_{tt}\|^2_W dt\right).\end{aligned} \tag{59}$$

Since $d_t \underline{\boldsymbol{e}}_{1,h}^n$ is not defined for $n = 0$, so we sum (59) over $n = 1, \cdots, m-1$ leading to

$$\begin{aligned}\|d_t \underline{\boldsymbol{e}}_{1,h}^m\|^2_0 + \Delta t \sum_{n=1}^{m-1} \|d_t \underline{\boldsymbol{e}}_{1,h}^{n+1}\|^2_W &\leq \|d_t \underline{\boldsymbol{e}}_{1,h}^1\|^2_0 + \left(\frac{5CC_p^2}{\nu} + \frac{5S_0 C\tilde{C}_p^2}{k_{\min}}\right)\left(\Delta t^2 \sum_{n=1}^{m-1} \int_{t^{n-1}}^{t^{n+1}} \|\underline{\boldsymbol{w}}_{ttt}\|^2_0 dt + \sum_{n=1}^{m-1} \int_{t^{n-1}}^{t^{n+1}} \|\underline{\xi}_{tt}\|^2_0 dt\right)\\
&\quad + \frac{5gCC_1C_2}{\nu k_{\min}}\Delta t^2 \sum_{n=1}^{m-1}\left(\int_{t^{n-1}}^{t^{n+1}} \|\underline{\xi}_{tt}\|^2_W dt + \int_{t^{n-1}}^{t^{n+1}} \|\underline{\boldsymbol{w}}_{tt}\|^2_W dt\right).\end{aligned} \tag{60}$$

Then, considering the regularity (51), as well as the property (22), we have

$$
\begin{aligned}
&\Delta t^2 \sum_{n=1}^{m-1} \int_{t^{n-1}}^{t^{n+1}} \|\underline{\boldsymbol{w}}_{ttt}\|_0^2 dt + \sum_{n=1}^{m-1} \int_{t^{n-1}}^{t^{n+1}} \|\underline{\boldsymbol{\xi}}_{tt}\|_0^2 dt \\
&\le \Delta t^2 \int_0^T \|\underline{\boldsymbol{w}}_{ttt}\|_0^2 dt + \int_0^T \|\underline{\boldsymbol{\xi}}_{tt}\|_0^2 dt \\
&\le C\Delta t^2 \left(\|\boldsymbol{u}_{ttt}\|^2_{L^2(0,T;L^2(\Omega_f))} + \|\varphi_{ttt}\|^2_{L^2(0,T;L^2(\Omega_p))} \right) + C\left(h^{2k_1} \|\boldsymbol{u}_{tt}\|^2_{L^2(0,T;H^{k_1}(\Omega_f))} + h^{2k_2} \|\varphi_{tt}\|^2_{L^2(0,T;H^{k_2}(\Omega_p))} \right),
\end{aligned}
$$

and

$$
\begin{aligned}
&\Delta t^2 \sum_{n=1}^{m-1} \left(\int_{t^{n-1}}^{t^{n+1}} \|\underline{\boldsymbol{\xi}}_{tt}\|_W^2 dt + \int_{t^{n-1}}^{t^{n+1}} \|\underline{\boldsymbol{w}}_{tt}\|_W^2 dt \right) \\
&\le \Delta t^2 \left(\int_0^T \|\underline{\boldsymbol{\xi}}_{tt}\|_W^2 dt + \int_0^T \|\underline{\boldsymbol{w}}_{tt}\|_W^2 dt \right) \\
&\le C\Delta t^2 \left(h^{2k_1-2} \|\boldsymbol{u}_{tt}\|^2_{L^2(0,T;H^{k_1}(\Omega_f))} + h^{2k_2-2} \|\varphi_{tt}\|^2_{L^2(0,T;H^{k_2}(\Omega_p))} + \|\boldsymbol{u}_{tt}\|^2_{L^2(0,T;H^{k_1}(\Omega_f))} + \|\varphi_{tt}\|^2_{L^2(0,T;H^{k_2}(\Omega_p))} \right) \\
&\le C\Delta t^2 \left(\|\boldsymbol{u}_{tt}\|^2_{L^2(0,T;H^{k_1}(\Omega_f))} + \|\varphi_{tt}\|^2_{L^2(0,T;H^{k_2}(\Omega_p))} \right), \quad k_1 \ge 1, k_2 \ge 1.
\end{aligned}
$$

Hence, we have

$$
\|d_t \underline{\boldsymbol{e}}_{1,h}^m\|_0^2 + \Delta t \sum_{n=1}^{m-1} \|d_t \underline{\boldsymbol{e}}_{1,h}^{n+1}\|_W^2 \le \|d_t \underline{\boldsymbol{e}}_{1,h}^1\|_0^2 + C(\nu, g, S_0, k_{\min}) \left(\Delta t^2 + h^{2k_1} + h^{2k_2} \right). \tag{61}
$$

In order to bound the term $\|d_t \underline{\boldsymbol{e}}_{1,h}^1\|_0$, we consider the error equation (55) in time t^1. Since $\underline{\boldsymbol{e}}_{1,h}^0 = (\boldsymbol{e}_{1,f}^0, e_{1,p}^0) = (\boldsymbol{0}, 0)$, we have $\underline{\boldsymbol{e}}_{1,h}^1 = \Delta t d_t \underline{\boldsymbol{e}}_{1,h}^1$. Then taking $\underline{\boldsymbol{z}}_h = 2 d_t \underline{\boldsymbol{e}}_{1,h}^1$ and $q_h = \epsilon_{1,h}^1$, a straightforward calculation gives

$$
\begin{aligned}
&2\|d_t \underline{\boldsymbol{e}}_{1,h}^1\|_0^2 + 2\Delta t \|d_t \underline{\boldsymbol{e}}_{1,h}^1\|_W^2 + 2\Delta t \sum_{i=1}^{d-1} \frac{\alpha\sqrt{\nu g}}{\sqrt{\mathrm{tr}(\boldsymbol{K})}} \|d_t \boldsymbol{e}_{1,f}^1 \cdot \tau_i\|^2_{L^2(\Gamma)} \\
&= 2\left[\underline{\boldsymbol{w}}_t^1 - \frac{\underline{\boldsymbol{w}}^1 - \underline{\boldsymbol{w}}^n}{\Delta t}, d_t \underline{\boldsymbol{e}}_{1,h}^1 \right] + 2\left[\frac{\underline{\boldsymbol{\xi}}^1 - \underline{\boldsymbol{\xi}}^0}{\Delta t}, d_t \underline{\boldsymbol{e}}_{1,h}^1 \right] - 2\Delta t a_\Gamma \left(\frac{\underline{\boldsymbol{\xi}}^1 - \underline{\boldsymbol{\xi}}^0}{\Delta t}, d_t \underline{\boldsymbol{e}}_{1,h}^1 \right) + 2\Delta t a_\Gamma \left(\frac{\underline{\boldsymbol{w}}^1 - \underline{\boldsymbol{w}}^0}{\Delta t}, d_t \underline{\boldsymbol{e}}_{1,h}^1 \right).
\end{aligned} \tag{62}
$$

Then, using the Hölder inequality, the Young's inequality and (18), we derive, $\forall \epsilon_2 > 0$,

$$
\begin{aligned}
&2\left[\underline{\boldsymbol{w}}_t^1 - \frac{\underline{\boldsymbol{w}}^1 - \underline{\boldsymbol{w}}^0}{\Delta t}, d_t \underline{\boldsymbol{e}}_{1,h}^1 \right] + 2\left[\frac{\underline{\boldsymbol{\xi}}^1 - \underline{\boldsymbol{\xi}}^0}{\Delta t}, d_t \underline{\boldsymbol{e}}_{1,h}^1 \right] \\
&\le 2\left\| \underline{\boldsymbol{w}}_t^1 - \frac{\underline{\boldsymbol{w}}^1 - \underline{\boldsymbol{w}}^0}{\Delta t} \right\|_0 \|d_t \underline{\boldsymbol{e}}_{1,h}^1\|_0 + 2\left\| \frac{\underline{\boldsymbol{\xi}}^1 - \underline{\boldsymbol{\xi}}^0}{\Delta t} \right\|_0 \|d_t \underline{\boldsymbol{e}}_{1,h}^1\|_0 \\
&\le 2\varepsilon_2 \|d_t \underline{\boldsymbol{e}}_{1,h}^1\|_0^2 + \frac{1}{\varepsilon_2} \left\| \underline{\boldsymbol{w}}_t^1 - \frac{\underline{\boldsymbol{w}}^1 - \underline{\boldsymbol{w}}^0}{\Delta t} \right\|_0^2 + \frac{1}{\varepsilon_2} \left\| \frac{\underline{\boldsymbol{\xi}}^1 - \underline{\boldsymbol{\xi}}^0}{\Delta t} \right\|_0^2 \\
&\le 2\varepsilon_2 \|d_t \underline{\boldsymbol{e}}_{1,h}^1\|_0^2 + \frac{C}{\varepsilon_2} \Delta t \int_{t^0}^{t^1} \|\underline{\boldsymbol{w}}_{tt}\|_0^2 dt + \frac{C}{\varepsilon_2 \Delta t} \int_{t^0}^{t^1} \|\underline{\boldsymbol{\xi}}_t\|_0^2 dt \\
&\le 2\varepsilon_2 \|d_t \underline{\boldsymbol{e}}_{1,h}^1\|_0^2 + \frac{C}{\varepsilon_2} \left(\Delta t^2 + h^{2k_1+2} + h^{2k_2+2} \right).
\end{aligned} \tag{63}
$$

From the definition of $a_\Gamma(\cdot,\cdot)$, we have

$$
-2\Delta t a_\Gamma \left(\frac{\underline{\boldsymbol{\xi}}^1 - \underline{\boldsymbol{\xi}}^0}{\Delta t}, d_t \underline{\boldsymbol{e}}_{1,h}^1 \right) = -2\Delta t g \int_\Gamma \left(\frac{\xi_p^1 - \xi_p^0}{\Delta t} \right) d_t \boldsymbol{e}_{1,f}^1 \cdot \boldsymbol{n}_f + 2\Delta t g \int_\Gamma d_t e_{1,p}^1 \left(\frac{\boldsymbol{\xi}_f^1 - \boldsymbol{\xi}_f^0}{\Delta t} \right) \cdot \boldsymbol{n}_f.
$$

Using the trace, Pincaré, inverse and Young's inequalities, we get

$$
-2\Delta t g \int_\Gamma \left(\frac{\xi_p^1 - \xi_p^0}{\Delta t} \right) d_t \boldsymbol{e}_{1,f}^1 \cdot \boldsymbol{n}_f \le 2\Delta t g C_t \tilde{C}_t \left\| \frac{\xi_p^1 - \xi_p^0}{\Delta t} \right\|_{\Omega_p}^{\frac{1}{2}} \left\| \nabla \left(\frac{\xi_p^1 - \xi_p^0}{\Delta t} \right) \right\|_{\Omega_p}^{\frac{1}{2}} \left\| d_t \boldsymbol{e}_{1,f}^1 \right\|_{\Omega_f}^{\frac{1}{2}} \left\| \nabla d_t \boldsymbol{e}_{1,f}^1 \right\|_{\Omega_f}^{\frac{1}{2}}
$$

$$
\begin{aligned}
&\le 2\Delta t g C_t \tilde{C}_t \cdot \tilde{C}_p^{\frac{1}{2}} \left\| \nabla \left(\frac{\xi_p^1 - \xi_p^0}{\Delta t} \right) \right\|_{\Omega_p} \cdot C_I^{\frac{1}{2}} h^{-\frac{1}{2}} \| d_t e_{1,f}^1 \|_{\Omega_f} \\
&\le \varepsilon_2 \| d_t \boldsymbol{e}_{1,f}^1 \|_{\Omega_f}^2 + \frac{g^2 C_t^2 \tilde{C}_t^2 \tilde{C}_p C_I}{\varepsilon_2 h} \Delta t^2 \left\| \nabla \left(\frac{\xi_p^1 - \xi_p^0}{\Delta t} \right) \right\|_{\Omega_p}^2 \\
&\le \varepsilon_2 \| d_t \boldsymbol{e}_{1,f}^1 \|_{\Omega_f}^2 + \frac{g^2 C_t^2 \tilde{C}_t^2 \tilde{C}_p C_I}{\varepsilon_2 h} \Delta t \int_{t^0}^{t^1} \| \nabla (\xi_p)_t \|_{\Omega_p}^2 dt \\
&\le \varepsilon_2 \| d_t \boldsymbol{e}_{1,f}^1 \|_{\Omega_f}^2 + \frac{C(g) \Delta t^2 h^{2k_2}}{\varepsilon_2 h} \le \varepsilon_2 \| d_t \boldsymbol{e}_{1,f}^1 \|_{\Omega_f}^2 + \frac{C(g)\Delta t^2}{\varepsilon_2}, \quad k_2 \ge 1.
\end{aligned}
$$

In way similar, we obtain

$$
\begin{aligned}
-2\Delta t g \int_\Gamma d_t e_{1,p}^1 \left(\frac{\xi_f^1 - \xi_f^0}{\Delta t} \right) \cdot \boldsymbol{n}_f &\le \varepsilon_2 g S_0 \| d_t e_{1,p}^1 \|_{\Omega_p}^2 + \frac{g C_t^2 \tilde{C}_t^2 C_p \tilde{C}_I}{\varepsilon_2 S_0 h} \Delta t^2 \left\| \nabla \left(\frac{\xi_f^1 - \xi_f^0}{\Delta t} \right) \right\|_{\Omega_f}^2 \\
&\le \varepsilon_2 g S_0 \| d_t e_{1,p}^1 \|_{\Omega_p}^2 + \frac{C(g, S_0) \Delta t^2 h^{2k_1}}{\varepsilon_2 h} \\
&\le \varepsilon_2 g S_0 \| d_t e_{1,p}^1 \|_{\Omega_p}^2 + \frac{C(g, S_0)\Delta t^2}{\varepsilon_2}, \quad k_1 \ge 1.
\end{aligned}
$$

So from the definition of $\|\cdot\|_0$ in (14), we get

$$
-2\Delta t a_\Gamma \left(\frac{\underline{\boldsymbol{\xi}}^1 - \underline{\boldsymbol{\xi}}^0}{\Delta t}, d_t \underline{\boldsymbol{e}}_{1,h}^1 \right) \le \varepsilon_2 \| d_t \underline{\boldsymbol{e}}_{1,h}^1 \|_0^2 + \frac{C(g, S_0)\Delta t^2}{\varepsilon_2}. \tag{64}
$$

Do the same estimates of (64), we have

$$
\begin{aligned}
&2\Delta t a_\Gamma \left(\frac{\underline{\boldsymbol{w}}^1 - \underline{\boldsymbol{w}}^0}{\Delta t}, d_t \underline{\boldsymbol{e}}_{1,h}^1 \right) = 2\Delta t g \int_\Gamma \left(\frac{\varphi^1 - \varphi^0}{\Delta t} \right) d_t e_{1,f}^1 \cdot \boldsymbol{n}_f - 2\Delta t g \int_\Gamma d_t e_{1,p}^1 \left(\frac{\boldsymbol{u}^1 - \boldsymbol{u}^0}{\Delta t} \right) \cdot \boldsymbol{n}_f \\
&\le \varepsilon_2 \| d_t \boldsymbol{e}_{1,f}^1 \|_{\Omega_f}^2 + \frac{g^2 C_t^2 \tilde{C}_t^2 \tilde{C}_p C_I}{\varepsilon_2 h} \Delta t \int_{t^0}^{t^1} \| \nabla \varphi_t \|_{\Omega_p}^2 dt + \varepsilon_2 g S_0 \| d_t e_{1,p}^1 \|_{\Omega_p}^2 + \frac{g C_t^2 \tilde{C}_t^2 C_p \tilde{C}_I}{\varepsilon_2 S_0 h} \Delta t \int_{t^0}^{t^1} \| \nabla \boldsymbol{u}_t \|_{\Omega_f}^2 dt \\
&\le \varepsilon_2 \| d_t \underline{\boldsymbol{e}}_{1,h}^1 \|_0^2 + \frac{C(g, S_0)\Delta t^2}{\varepsilon_2 h}.
\end{aligned} \tag{65}
$$

A combination of estimates (63)-(65) and (62) along with $\varepsilon_2 = 1/4$ gives

$$
\| d_t \underline{\boldsymbol{e}}_{1,h}^1 \|_0^2 + \Delta t \| d_t \underline{\boldsymbol{e}}_{1,h}^1 \|_W^2 \le C(g, S_0) \left(\Delta t^2 + h^{2k_1+2} + h^{2k_2+2} + \frac{\Delta t^2}{h} \right). \tag{66}
$$

From the estimates (66) and (61), we get

$$
\| d_t \underline{\boldsymbol{e}}_{1,h}^m \|_0^2 + \Delta t \sum_{n=0}^{m-1} \| d_t \underline{\boldsymbol{e}}_{1,h}^{n+1} \|_W^2 \le C(\nu, g, S_0, k_{\min}) \left(\Delta t^2 + h^{2k_1} + h^{2k_2} + \frac{\Delta t^2}{h} \right).
$$

This completes the proof. □

We now give the error estimates for the Para-SDC decoupled algorithm.

Theorem 5.1. *Under the assumptions of Lemma 5.2, we have*

$$
\| \underline{\boldsymbol{e}}_{2,h}^m \|_0^2 + \Delta t \sum_{n=0}^{m-1} \| \underline{\boldsymbol{e}}_{2,h}^{n+1} \|_W^2 \le C\left(d, \alpha, \nu, g, S_0, k_{\min} \right) \left(\Delta t^4 + h^{2k_1+2} + h^{2k_2+2} + \frac{\Delta t^4}{h} \right). \tag{67}
$$

Proof. Considering the equation (15) for the time of t^n and t^{n+1}, then calculate the mean of them resulting in

$$
\begin{cases}
\frac{1}{2}\left[\underline{\boldsymbol{w}}_t^{n+1} + \underline{\boldsymbol{w}}_t^n, \underline{\boldsymbol{z}} \right] + \frac{1}{2} a\left(\underline{\boldsymbol{w}}^{n+1} + \underline{\boldsymbol{w}}^n, \underline{\boldsymbol{z}} \right) + \frac{1}{2} a_\Gamma \left(\underline{\boldsymbol{w}}^{n+1} + \underline{\boldsymbol{w}}^n, \underline{\boldsymbol{z}} \right) + \frac{1}{2} b\left(\underline{\boldsymbol{z}}, p^{n+1} + p^n \right) = \frac{1}{2}\left(\boldsymbol{f}^{n+1} + \boldsymbol{f}^n, \underline{\boldsymbol{z}} \right), \quad \forall \underline{\boldsymbol{z}} \in \boldsymbol{W}, \\
b\left(\underline{\boldsymbol{w}}^{n+1} + \underline{\boldsymbol{w}}^n, q \right) = 0, \quad \forall q \in Q.
\end{cases}
$$

Then, subtracting it from (39), and considering (21) and (47), we have the following errors equations:

$$\begin{cases}\left[\frac{\underline{e}_{2,h}^{n+1}-\underline{e}_{2,h}^{n}}{\Delta t},\underline{z}_h\right]+a\left(\underline{e}_{2,h}^{n+1},\underline{z}_h\right)+a_\Gamma\left(\underline{e}_{2,h}^{n},\underline{z}_h\right)+b\left(\underline{z}_h,\epsilon_{2,h}^{n+1}\right)=\left[\frac{\underline{w}_t^{n+1}+\underline{w}_t^{n}}{2}-\frac{\underline{w}^{n+1}-\underline{w}^{n}}{\Delta t},\underline{z}_h\right]+\left[\frac{\underline{\xi}^{n+1}-\underline{\xi}^{n}}{\Delta t},\underline{z}_h\right]\\ \quad +a\left(\frac{\underline{e}_{1,h}^{n+1}-\underline{e}_{1,h}^{n}}{2},\underline{z}_h\right)-a_\Gamma\left(\frac{\underline{e}_{1,h}^{n+1}-\underline{e}_{1,h}^{n}}{2},\underline{z}_h\right)+b\left(\underline{z}_h,\frac{\epsilon_{1,h}^{n+1}-\epsilon_{1,h}^{n}}{2}\right),\\ b\left(\underline{e}_{2,h}^{n+1},q_h\right)=0.\end{cases} \tag{68}$$

Setting $\underline{z}_h=2\Delta t\underline{e}_{2,h}^{n+1}$ in (68) yields

$$\begin{aligned}&\|\underline{e}_{2,h}^{n+1}\|_0^2-\|\underline{e}_{2,h}^{n}\|_0^2+\|\underline{e}_{2,h}^{n+1}-\underline{e}_{2,h}^{n}\|_0^2+2\Delta t\|\underline{e}_{2,h}^{n+1}\|_W^2+2\Delta t\sum_{i=1}^{d-1}\frac{\alpha\sqrt{\nu g}}{\sqrt{\operatorname{tr}(\boldsymbol{K})}}\|\underline{e}_{2,h}^{n+1}\cdot\tau_i\|_{L^2(\Gamma)}^2\\&=2\Delta t\left[\frac{\underline{w}_t^{n+1}+\underline{w}_t^{n}}{2}-\frac{\underline{w}^{n+1}-\underline{w}^{n}}{\Delta t}+\frac{\underline{\xi}^{n+1}-\underline{\xi}^{n}}{\Delta t},\underline{e}_{2,h}^{n+1}\right]-2\Delta t a_\Gamma\left(\underline{e}_{2,h}^{n},\underline{e}_{2,h}^{n+1}\right)+\Delta t^2a\left(d_t\underline{e}_{1,h}^{n+1},\underline{e}_{2,h}^{n+1}\right)-\Delta t^2a_\Gamma\left(d_t\underline{e}_{1,h}^{n+1},\underline{e}_{2,h}^{n+1}\right).\end{aligned} \tag{69}$$

In a similar way to the estimation of (58), we get

$$\begin{aligned}&2\Delta t\left[\frac{\underline{w}_t^{n+1}+\underline{w}_t^{n}}{2}-\frac{\underline{w}^{n+1}-\underline{w}^{n}}{\Delta t}+\frac{\underline{\xi}^{n+1}-\underline{\xi}^{n}}{\Delta t},\underline{e}_{2,h}^{n+1}\right]\\&\le 2\varepsilon\Delta t\|\underline{e}_{2,h}^{n+1}\|_W^2+\left(\frac{C_p^2}{\varepsilon\nu}+\frac{S_0\tilde{C}_p^2}{\varepsilon k_{\min}}\right)\Delta t\left(\left\|\frac{\underline{w}_t^{n+1}+\underline{w}_t^{n}}{2}-\frac{\underline{w}^{n+1}-\underline{w}^{n}}{\Delta t}\right\|_0^2+\left\|\frac{\underline{\xi}^{n+1}-\underline{\xi}^{n}}{\Delta t}\right\|_0^2\right).\end{aligned}$$

By applying the property (16) and the estimation (31), we have

$$\begin{aligned}-2\Delta t a_\Gamma\left(\underline{e}_{2,h}^{n},\underline{e}_{2,h}^{n+1}\right)&=2\Delta t a_\Gamma\left(\underline{e}_{2,h}^{n+1}-\underline{e}_{2,h}^{n},\underline{e}_{2,h}^{n+1}\right)\\&\le\varepsilon\Delta t\|\underline{e}_{2,h}^{n+1}\|_W^2+\frac{gC_1}{\varepsilon h}\max\left\{\frac{\tilde{C}_pC_I}{k_{\min}},\frac{C_p\tilde{C}_I}{\nu S_0}\right\}\Delta t\|\underline{e}_{2,h}^{n+1}-\underline{e}_{2,h}^{n}\|_0^2.\end{aligned}$$

Similar to the bound (44), we have

$$\begin{aligned}&\Delta t^2a\left(d_t\underline{e}_{1,h}^{n+1},\underline{e}_{2,h}^{n+1}\right)=\Delta t^2a_f\left(d_te_{1,f}^{n+1},e_{2,f}^{n+1}\right)+\Delta t^2a_p\left(d_te_{1,p}^{n+1},e_{2,p}^{n+1}\right)\\&\le\varepsilon\Delta t\|\underline{e}_{2,h}^{n+1}\|_W^2+\varepsilon\Delta t\sum_{i=1}^{d-1}\frac{\alpha\sqrt{\nu g}}{\sqrt{\operatorname{tr}(\boldsymbol{K})}}\|e_{2,f}^{n+1}\cdot\tau_i\|_{L^2(\Gamma)}^2+\left(\frac{1}{4\varepsilon}+\frac{C_t^2C_p(d-1)\alpha g}{4\varepsilon\sqrt{\nu g k_{\min}}}\right)\Delta t^3\|d_t\underline{e}_{1,h}^{n+1}\|_W^2.\end{aligned}$$

We bound the last term on the right hand side of (69) by using (16) and (29),

$$-\Delta t^2a_\Gamma\left(d_t\underline{e}_{1,h}^{n+1},\underline{e}_{2,h}^{n+1}\right)=\Delta t^2a_\Gamma\left(\underline{e}_{2,h}^{n+1},d_t\underline{e}_{1,h}^{n+1}\right)\le\varepsilon\Delta t\|\underline{e}_{2,h}^{n+1}\|_W^2+\frac{gC_1C_2}{4\varepsilon\nu k_{\min}}\Delta t^3\|d_t\underline{e}_{1,h}^{n+1}\|_W^2.$$

Under the condition (49), combining these above estimates with (69) and taking $\varepsilon=1/5$ lead to

$$\begin{aligned}\|\underline{e}_{2,h}^{n+1}\|_0^2-\|\underline{e}_{2,h}^{n}\|_0^2+\Delta t\|\underline{e}_{2,h}^{n+1}\|_W^2\le&\left(\frac{5C_p^2}{\nu}+\frac{5S_0\tilde{C}_p^2}{k_{\min}}\right)\Delta t\left(\left\|\frac{\underline{w}_t^{n+1}+\underline{w}_t^{n}}{2}-\frac{\underline{w}^{n+1}-\underline{w}^{n}}{\Delta t}\right\|_0^2+\left\|\frac{\underline{\xi}^{n+1}-\underline{\xi}^{n}}{\Delta t}\right\|_0^2\right)\\&+\left(\frac{5}{4}+\frac{5C_t^2C_p(d-1)\alpha g}{4\sqrt{\nu g k_{\min}}}+\frac{5gC_1C_2}{4\nu k_{\min}}\right)\Delta t^3\|d_t\underline{e}_{1,h}^{n+1}\|_W^2.\end{aligned} \tag{70}$$

Note that $\underline{e}_{2,h}^0=\underline{w}_{2,h}^0-P_h^{w}\underline{w}^0=\mathbf{0}$. Summing (70) up from $n=0,1,\cdots,m-1$, results in

$$\begin{aligned}\|\underline{e}_{2,h}^{m}\|_0^2+\Delta t\sum_{n=0}^{m-1}\|\underline{e}_{2,h}^{n+1}\|_W^2\le&\left(\frac{5C_p^2}{\nu}+\frac{5S_0\tilde{C}_p^2}{k_{\min}}\right)\Delta t\sum_{n=0}^{m-1}\left(\left\|\frac{\underline{w}_t^{n+1}+\underline{w}_t^{n}}{2}-\frac{\underline{w}^{n+1}-\underline{w}^{n}}{\Delta t}\right\|_0^2+\left\|\frac{\underline{\xi}^{n+1}-\underline{\xi}^{n}}{\Delta t}\right\|_0^2\right)\\&+\left(\frac{5}{4}+\frac{5C_t^2C_p(d-1)\alpha g}{4\sqrt{\nu g k_{\min}}}+\frac{5gC_1C_2}{4\nu k_{\min}}\right)\Delta t^3\sum_{n=0}^{m-1}\|d_t\underline{e}_{1,h}^{n+1}\|_W^2.\end{aligned} \tag{71}$$

Applying the Hölder inequality and the regularities (51), we have

$$\begin{aligned}
&\Delta t\sum_{n=0}^{m-1}\left\|\frac{\underline{\boldsymbol{w}}_t^{n+1}+\underline{\boldsymbol{w}}_t^{n}}{2}-\frac{\underline{\boldsymbol{w}}^{n+1}-\underline{\boldsymbol{w}}^{n}}{\Delta t}\right\|_0^2=\Delta t\sum_{n=0}^{m-1}\left\|\frac{\underline{\boldsymbol{w}}_t^{n+1}+\underline{\boldsymbol{w}}_t^{n}}{2}-\frac{1}{\Delta t}\int_{t^n}^{t^{n+1}}\underline{\boldsymbol{w}}_t dt\right\|_0^2\\
&\le \Delta t\sum_{n=0}^{m-1}\left\|\frac{1}{2\Delta t}\int_{t^n}^{t^{n+1}}(t-t^n)(t-t^{n+1})\underline{\boldsymbol{w}}_{ttt}dt\right\|_0^2\\
&\le \frac{1}{\Delta t}\sum_{n=0}^{m-1}\left(\int_{t^n}^{t^{n+1}}(t-t^n)^2(t-t^{n+1})^2dt\right)\left(\int_{t^n}^{t^{n+1}}\|\underline{\boldsymbol{w}}_{ttt}\|_0^2dt\right)\\
&\le C\Delta t^4\sum_{n=0}^{m-1}\int_{t^n}^{t^{n+1}}\|\underline{\boldsymbol{w}}_{ttt}\|_0^2dt\le C\Delta t^4\left(\|\boldsymbol{u}_{ttt}\|^2_{L^2(0,T;L^2(\Omega_f))}+\|\varphi_{ttt}\|^2_{L^2(0,T;L^2(\Omega_p))}\right).
\end{aligned} \tag{72}$$

In addition, from (22) and (48), we have

$$\begin{aligned}
\Delta t\sum_{n=0}^{m-1}\left\|\frac{\underline{\xi}^{n+1}-\underline{\xi}^{n}}{\Delta t}\right\|_0^2&=\Delta t\sum_{n=0}^{m-1}\left\|\frac{1}{\Delta t}\int_{t^n}^{t^{n+1}}1\cdot\underline{\xi}_t dt\right\|_0^2\le C\sum_{n=0}^{m-1}\int_{t^n}^{t^{n+1}}\|\underline{\xi}_t\|_0^2dt\\
&\le C\left(h^{2k_1+2}\|\boldsymbol{u}_t\|^2_{L^2(0,T;H^{k_1+1}(\Omega_f))}+h^{2k_2+2}\|\varphi_t\|^2_{L^2(0,T;H^{k_2+1}(\Omega_p))}\right).
\end{aligned} \tag{73}$$

Now applying the bounds given by (33), (72) and (73), the estimate (71) becomes

$$\|\underline{\boldsymbol{e}}_{2,h}^m\|_0^2+\Delta t\sum_{n=0}^{m-1}\|\underline{\boldsymbol{e}}_{2,h}^{n+1}\|_W^2\le C\left(d,\alpha,\nu,g,S_0,k_{\min}\right)\left(\Delta t^4+h^{2k_1+2}+h^{2k_2+2}+\frac{\Delta t^4}{h}\right),\quad k_1,k_2\ge 1.$$

This completes the proof of theorem. □

By utilizing the approximation properties (22), along with Theorem 5.1 and the triangle inequalities, we can derive the following results immediately.

Theorem 5.2. *Under the assumption of Theorem 5.1, then we have*

$$\|\underline{\boldsymbol{w}}_{2,h}^m-\underline{\boldsymbol{w}}^m\|_0^2\le C\left(d,\alpha,\nu,g,S_0,k_{\min}\right)\left(\Delta t^4+h^{2k_1+2}+h^{2k_2+2}+\frac{\Delta t^4}{h}\right). \tag{74}$$

6. Numerical experiments

There are three numerical experiments in this section to demonstrate the reliability and effectiveness of Algorithm 3.1. First, we examine the convergence rate in order to illustrate the accuracy of our scheme. The second test verifies the stability for the smaller parameters ν, S_0 and $k_{\min}$. In the final experiment, we compare different schemes based on the second-order SDC method, demonstrating that our Para-SDC decoupled scheme achieves comparable accuracy to other coupled or serial schemes while significantly reducing CPU time consumption.

6.1. Convergence rates

Let the computational domain $\Omega\subset\mathbb{R}^2$, with $\Omega_f=(0,1)\times(1,2)$, $\Omega_p=(0,1)\times(0,1)$ and the interface $\Gamma=(0,1)\times\{1\}$. We take the exact solution:

$$\begin{cases}
\boldsymbol{u}(x,y,t)=\left(\left(x^2(y-1)^2+y\right)\cos(t),\left(-\frac{2}{3}x(y-1)^3+2-\pi\sin(\pi x)\right)\cos(t)\right),\\
p(x,y,t)=(2-\pi\sin(\pi x))\sin\left(\frac{\pi}{2}y\right)\cos(t),\\
\varphi(x,y,t)=(2-\pi\sin(\pi x))(1-y-\cos(\pi y))\cos(t)+\frac{1}{2}\left(1+(2-\pi\sin(\pi x))^2\right)\left((y-1)^2+1\right)\cos^2(t).
\end{cases}$$

For simplicity, we assume that all the physical parameters α, g, ν and S_0 are set to 1.0 and the hydraulic conductivity tensor $\boldsymbol{K}=K\boldsymbol{I}=\boldsymbol{I}$. The initial conditions, the boundary conditions and the right-hand side source terms follow from the above exact solutions. The finite element spaces used for the spatial discretization: the MINI elements ($P1b-P1$) to the Stokes problem, and the piecewise linear Lagrange elements (P_1) to the Darcy problem. And all tests in this paper are implemented by the software package FreeFem++.

In order to examine the spatial and temporal convergence rates by the varying mesh size h and time step Δt for Algorithm 3.1, we utilize the measure of convergence in [21], which can efficiently avoid the interaction between Δt and h in the convergence tests. Assume that $v_h^{\Delta t}(x,t_m)\approx v(x,t_m)+C_1(x,t_m)\Delta t^{\gamma}+C_2(x,t_m)h^{\mu}$, let us define the measures to examine the orders to convergence with respect to the mesh size h and the time step Δt as follows:

Table 1
Convergence orders of Algorithm 3.1 with varying time step Δt but fixed spacing $h = 1/8$.

Δt	$\|\boldsymbol{u}^m_{2,\Delta t} - \boldsymbol{u}^m_{2,\frac{\Delta t}{2}}\|_{0,\Omega_f}$	$\rho_{\boldsymbol{u},\Delta t,0}$	$\|\boldsymbol{u}^m_{2,\Delta t} - \boldsymbol{u}^m_{2,\frac{\Delta t}{2}}\|_{1,\Omega_f}$	$\rho_{\boldsymbol{u},\Delta t,1}$	$\|p^m_{2,\Delta t} - p^m_{2,\frac{\Delta t}{2}}\|_{\Omega_f}$	$\rho_{p,\Delta t,0}$
1/80	6.3298e-7	3.9738	3.8077e-6	3.9762	2.0317e-5	3.7878
1/160	1.5929e-7	3.9869	9.5763e-7	3.9878	5.3638e-6	3.8929
1/320	3.9953e-8	3.9933	2.4014e-7	3.9939	1.3779e-6	3.9463
1/640	1.0005e-8		6.0127e-8		3.4915e-7	
Δt	$\|\varphi^m_{2,\Delta t} - \varphi^m_{2,\frac{\Delta t}{2}}\|_{0,\Omega_p}$	$\rho_{\varphi,\Delta t,0}$	$\|\varphi^m_{2,\Delta t} - \varphi^m_{2,\frac{\Delta t}{2}}\|_{1,\Omega_p}$	$\rho_{\varphi,\Delta t,1}$		
1/80	1.1466e-5	4.0025	4.3678e-5	4.0044		
1/160	2.8646e-6	4.0015	1.0907e-5	4.0024		
1/320	7.1588e-7	4.0008	2.7252e-6	4.0012		
1/640	1.7893e-7		6.8110e-7			

Table 2
Convergence orders of Algorithm 3.1 with varying mesh h but fixed time step $\Delta t = 1/20$.

h	$\|\boldsymbol{u}^m_{2,h} - \boldsymbol{u}^m_{2,\frac{h}{2}}\|_{0,\Omega_f}$	$\rho_{\boldsymbol{u},h,0}$	$\|\boldsymbol{u}^m_{2,h} - \boldsymbol{u}^m_{2,\frac{h}{2}}\|_{1,\Omega_f}$	$\rho_{\boldsymbol{u},h,1}$	$\|p^m_{2,h} - p^m_{2,\frac{h}{2}}\|_{0,\Omega_f}$	$\rho_{p,h,0}$
1/8	1.3854e-2	3.9855	3.4879e-1	2.0380	1.0246e-1	2.9437
1/16	3.4760e-3	3.9925	1.7114e-1	2.0742	3.4808e-2	2.7994
1/32	8.7065e-4	3.9792	8.2509e-2	2.1704	1.2434e-2	2.7088
1/64	2.1880e-4		3.8016e-2		4.5903e-3	
h	$\|\varphi^m_{2,h} - \varphi^m_{2,\frac{h}{2}}\|_{0,\Omega_p}$	$\rho_{\varphi,h,0}$	$\|\varphi^m_{2,h} - \varphi^m_{2,\frac{h}{2}}\|_{1,\Omega_p}$	$\rho_{\varphi,h,1}$		
1/8	3.4220e-2	3.9709	9.0197e-1	2.0373		
1/16	8.6178e-3	3.9927	4.4273e-1	2.0957		
1/32	2.1584e-3	3.9986	2.1126e-1	2.2346		
1/64	5.3978e-4		9.4538e-2			

$$\rho_{v,h,i} = \frac{\| v_h^{\Delta t}(x,t_m) - v_{\frac{h}{2}}^{\Delta t}(x,t_m) \|_{i,D}}{\| v_{\frac{h}{2}}^{\Delta t}(x,t_m) - v_{\frac{h}{4}}^{\Delta t}(x,t_m) \|_{i,D}} \approx \frac{4^\mu - 2^\mu}{2^\mu - 1},$$

$$\rho_{v,\Delta t,i} = \frac{\| v_h^{\Delta t}(x,t_m) - v_h^{\frac{\Delta t}{2}}(x,t_m) \|_{i,D}}{\| v_h^{\frac{\Delta t}{2}}(x,t_m) - v_h^{\frac{\Delta t}{4}}(x,t_m) \|_{i,D}} \approx \frac{4^\gamma - 2^\gamma}{2^\gamma - 1}.$$

Here v refers to $\boldsymbol{u}, p$ or φ, D denotes Ω_f or Ω_p, and i can be 0 and 1 representing the L^2-norm and H^1-norm, respectively. Specially, if $\rho_{v,h,0}$ and $\rho_{v,\Delta t,0}$ approach 4.0 for $\mu = \gamma = 2$, the corresponding order of convergence in space and time will be of $O(h^2)$ and $O(\Delta t^2)$, respectively.

First, we test the order of convergence with respect to the time step Δt, and we set a fixed mesh size $h = 1/8$ and the varying time step Δt. Table 1 show the temporal convergence performances of the velocity $\boldsymbol{u}$, pressure p and the piezometric head φ for Algorithm 3.1 at time $t^m = 1.0$. Since all the parameter $\rho_{\cdot,\Delta t,i} \approx 4.0$, $i = 0, 1$, the convergence orders in time are $O(\Delta t^2)$. These numerical results illustrate the second-order convergence of Algorithm 3.1. In Table 2, we list the results of convergence orders with respect to h, with a fixed time step $\Delta t = 1/20$ and varying spacing h. These results display that the error estimates $O(h^2)$ for the L^2-norm of $\boldsymbol{u}^m_{2,h}$ and $\varphi^m_{2,h}$, $O(h)$ for the H^1-norm of $\boldsymbol{u}^m_{2,h}$ and $\varphi^m_{2,h}$, and the L^2-norm of $p^m_{2,h}$ is optimal in space for Algorithm 3.1.

6.2. Stability for the smaller parameters

Since the Para-SDC decoupled algorithm is stable under a time step restriction (32), we then check the stability of it with the smaller parameters, such as ν, S_0 and K. To test the effects of the smaller parameters on the stability, we define the quality of energy $E(t^m) = \|\boldsymbol{u}^m_{2,h}\|^2_{\Omega_f} + gS_0\|\varphi^m_{2,h}\|^2_{\Omega_p}$. Choose the source terms $\boldsymbol{f}_1 = \boldsymbol{0}$ and $f_2 = 0$, the initial values $\boldsymbol{u}^0 = \boldsymbol{1}$ and $\varphi^0 = 1$. We set all physical parameters to 1 except ν, S_0 and K. Due to the hydraulic conductivity tensor are set to $\boldsymbol{K} = K\boldsymbol{I}$, $k_{\min}$ in (18) is equal to the hydraulic conductivity variable K. Fig. 1 displays the quantity of energy $E(t^m)$ with the smaller parameters ν, S_0 and $k_{\min}$, respectively. Apparently, our decoupled scheme is still stable even for much smaller $\nu, S_0, k_{\min}$ than our stability analysis predicted.

6.3. Comparisons of varied second-order methods

In order to demonstrate the effectiveness of the decoupled and parallel techniques for Algorithm 3.1, we evaluate our scheme against various algorithms that based on the second-order SDC method. For example, the second-order SDC algorithm [43], and the Para/SDC algorithm [42] which is based on the parareal and second-order SDC methods. However, these two schemes solve the mixed Stokes/Darcy model directly. Furthermore, we present the second-order decoupled algorithm based on SDC method in Algorithm 6.1, as a reference to highlight the parallel efficiency of our Para-SDC decoupled algorithm.

Algorithm 6.1. *(SDC Decoupled Algorithm)*

Step 1. *Using the first-order decoupled scheme (23) to get* $\left(\underline{\boldsymbol{w}}^{n+1}_{1,h}, p^{n+1}_{1,h}\right)$ *with* $n = 0, \ldots, N-1$.

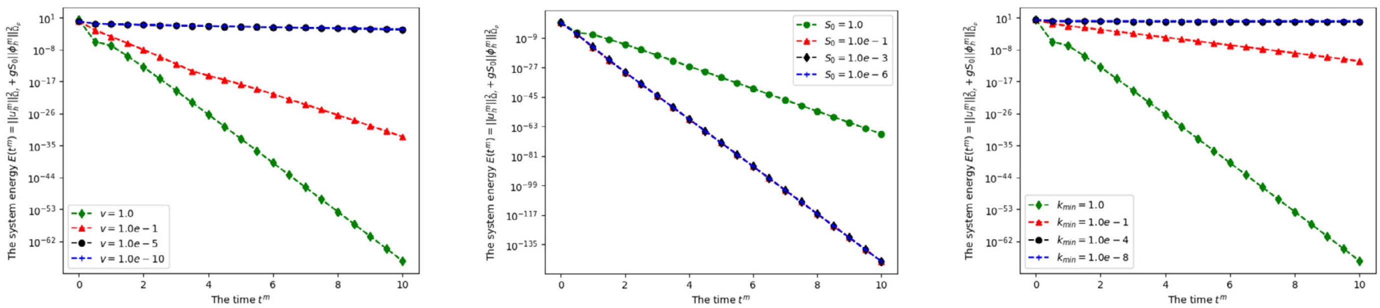

(a) $S_0 = k_{\min} = 1.0$ (b) $\nu = k_{\min} = 1.0$ (c) $\nu = S_0 = 1.0$

Fig. 1. Energy of Algorithm 3.1 on the time step points t^m with fixed $\Delta t = 1/10$ and $h = 1/32$.

Table 3
Comparisons of the various second-order algorithms based on SDC method.

Numerical Algorithms	$h = 1/16$			$h = 1/128$		
	Error	CPU(s)	Speedup	Error	CPU(s)	Speedup
SDC	1.5545e-2	17.312	-	1.3579e-3	1037.23	-
SDC Decoupled	1.5546e-2	10.696	-	1.3585e-3	663.394	-
Para-SDC	1.5545e-2	6.470	2.676	1.3579e-3	423.412	2.450
Para-SDC Decoupled	1.5546e-2	4.059	4.265	1.3585e-3	268.229	3.867

Step 2. *Using the second-order SDC method to compute* $(\boldsymbol{w}_D^{n+1}, p_D^{n+1}) \in \boldsymbol{W}_h \times Q_h$ *such that* $\forall\, (\underline{\boldsymbol{z}}_h, q_h) \in \boldsymbol{W}_h \times Q_h$,

$$\begin{cases} \left[\dfrac{\boldsymbol{w}_D^{n+1} - \boldsymbol{w}_D^n}{\Delta t}, \underline{\boldsymbol{z}}_h\right] + a\left(\boldsymbol{w}_D^{n+1}, \underline{\boldsymbol{z}}_h\right) + b\left(\underline{\boldsymbol{z}}_h, p_D^{n+1}\right) \\ \quad = -a_\Gamma\left(\boldsymbol{w}_D^n, \underline{\boldsymbol{z}}_h\right) + a\left(\dfrac{\boldsymbol{w}_{1,h}^{n+1} - \boldsymbol{w}_{1,h}^n}{2}, \underline{\boldsymbol{z}}_h\right) - a_\Gamma\left(\dfrac{\boldsymbol{w}_{1,h}^{n+1} - \boldsymbol{w}_{1,h}^n}{2}, \underline{\boldsymbol{z}}_h\right) + b\left(\underline{\boldsymbol{z}}_h, \dfrac{p_{1,h}^{n+1} - p_{1,h}^n}{2}\right) + \left(\dfrac{\boldsymbol{f}^{n+1} + \boldsymbol{f}^n}{2}, \underline{\boldsymbol{z}}_h\right), \\ b\left(\boldsymbol{w}_D^{n+1}, q_h\right) = 0. \end{cases}$$

We will display the errors between the exact solutions and the numerical solutions, along with the Central Processing Unit (CPU) time for the various second-order schemes. In addition, to quantitatively measure the parallel efficiency, let us define the parallel speedup as the ratio between the serial with parallel cost. Let us calculate the parallel speedup of Algorithm 3.1. Assume that there are $2N$ processors can be allocated to the N sub-intervals $[t^n, t^{n+1}]$, $n = 0, 1, \cdots, N-1$. Therefore, each time step will be assigned two processors, such as the processors P_{2n} and P_{2n+1} are assigned to the subinterval $[t^n, t^{n+1}]$. Hence, we are capable to solve these two decoupled sub-problems over each time step concurrently. Let us denote $\Upsilon_{G,S}$ and $\Upsilon_{F,S}$ as the numerical cost of one processor to compute the decoupled Stokes equations over one time step based on the $\mathscr{G}$ and $\mathscr{F}$, respectively. In the same way, we denote $\Upsilon_{G,D}$ and $\Upsilon_{F,D}$ as the corresponding cost for the decoupled Darcy equations. Notice that the computational cost of the Stokes equations is greater than that of the Darcy equations. Assume that all processors are homogeneous and the communication delays between them are negligible. Hence, following the pipelined version [44] of parareal method, the total cost of the Para-SDC decoupled algorithm for one iteration with $2N$ processors equals

$$\begin{aligned} &N \cdot \max\{\Upsilon_{G,S}, \Upsilon_{G,D}\} + \left(\max\{\Upsilon_{F,S}, \Upsilon_{F,D}\} + \max\{\Upsilon_{G,S}, \Upsilon_{G,D}\}\right) \\ &= N\Upsilon_{G,S} + \left(\Upsilon_{F,S} + \Upsilon_{G,S}\right) = (N+1)\Upsilon_{G,S} + \Upsilon_{F,S}. \end{aligned}$$

What's more, the computational cost of the serial second-order SDC method is $N(\Upsilon_G + \Upsilon_F)$, where Υ_G and Υ_F represent the cost for one processor to compute one time step of $\mathscr{G}$ and $\mathscr{F}$, respectively. Hence, the parallel speedup of Algorithm 3.1 is $\frac{N(\Upsilon_G+\Upsilon_F)}{(N+1)\Upsilon_{G,S}+\Upsilon_{F,S}}$. Following a similar process, we can obtain that the parallel speedup of Para-SDC algorithm [42] is equal to $\frac{N(\Upsilon_G+\Upsilon_F)}{(N+1)\Upsilon_G+\Upsilon_F}$, which is obviously less than that of Algorithm 3.1.

We consider the same computational domain, triangulation and exact solutions of the test as in Section 6.1. Let us take the fixed time step size $\Delta t = 1/100$ and varying spacing $h = 1/16, 1/128$. In Table 3, we provide the errors between the exact solutions and the numerical solutions, CPU time and the parallel speedup of different algorithms. From the data in Table 3, it is easy to see that our Para-SDC decoupled scheme almost retains the same accuracy as the other schemes, but owns the least CPU time and the highest parallel speedup. Accordingly, the decoupled and parallel techniques in our scheme do not degrade approximation accuracy, but they improve the computational efficiency significantly.

7. Conclusions

This article proposes and analyses a second-order time parallel decoupled algorithm for the unsteady mixed Stokes/Darcy model. It is able to effectively improve the computational efficiency in solving the coupling problems, as well as take full advantage of the abundant parallel computing resources available today. The stability and convergence results are evaluated under some time step limitations. Numerical experiments are conducted to demonstrate the computational accuracy, stability and efficiency of our algorithm. The future work is promising in extending this approach to nonlinear cases in the fluid part, or even the phase field model of the coupled two-phase free flow and two-phase porous media flow.

Data availability

No data was used for the research described in the article.

Acknowledgements

This work is supported by the National Natural Science Foundation of China (Nos. 11971378 and 12101494), the Natural Science Foundation of Shaanxi Province (No. 2021JQ-426) and the Scientific Research Program funded by Education Department of Shaanxi Provincial Government (No. 21JK0935).

References

[1] W.J. Layton, F. Schieweck, I. Yotov, Coupling fluid flow with porous media flow, SIAM J. Numer. Anal. 40 (6) (2002) 2195–2218.
[2] Y. Cao, M. Gunzburger, F. Hua, X. Wang, Coupled Stokes-Darcy model with Beavers-Joseph interface boundary condition, Commun. Math. Sci. 8 (2010) (2010) 1–25.
[3] M. Discacciati, A. Quarteroni, Navier-Stokes/Darcy coupling: modeling, analysis, and numerical approximation, Rev. Mat. Complut. 22 (2) (2009) 315–426.
[4] Q. Li, G. Du, Local and parallel finite element methods based on two-grid discretizations for a transient coupled Navier-Stokes/Darcy model, J. Sci. Comput. 92 (3) (2022).
[5] Y. Hou, D. Xue, Numerical analysis of two-grid decoupling finite element scheme for Navier-Stokes/Darcy model, Comput. Math. Appl. 113 (2022) 45–51.
[6] J. Yue, J. Li, Efficient coupled deep neural networks for the time-dependent coupled Stokes-Darcy problems, Appl. Math. Comput. 437 (2023).
[7] Bin Zhao, Mingyue Zhang, Chuangchuang Liang, Global well-posedness for Navier-Stokes-Darcy equations with the free interface, Int. J. Numer. Anal. Model. 18 (5) (2021) 569–619.
[8] Feng Shi, Yizhong Sun, Haibiao Zheng, Ensemble domain decomposition algorithm for the fully mixed random Stokes-Darcy model with the Beavers-Joseph interface conditions, SIAM J. Numer. Anal. 61 (3) (2023) 1482–1512.
[9] M. Mu, M. Cai, A multilevel decoupled method for a mixed Stokes/Darcy model, J. Comput. Appl. Math. 236 (9) (2012) 2452–2465.
[10] M. Mu, J. Xu, A two-grid method of a mixed Stokes-Darcy model for coupling fluid flow with porous media flow, SIAM J. Numer. Anal. 45 (5) (2007) 1801–1813.
[11] Michaela Kubacki, Marina Moraiti, Analysis of a second-order, unconditionally stable, partitioned method for the evolutionary Stokes-Darcy model, Int. J. Numer. Anal. Model. 12 (4) (2015) 704–730.
[12] G. Fu, C. Lehrenfeld, A strongly conservative hybrid DG/Mixed FEM for the coupling of Stokes and Darcy flow, J. Sci. Comput. 77 (3) (2018) 1605–1620.
[13] K.E. Holter, M. Kuchta, K.-A. Mardal, Robust preconditioning for coupled Stokes-Darcy problems with the Darcy problem in primal form, Comput. Math. Appl. 91 (2021) 53–66.
[14] W. Chen, M. Gunzburger, S. Dong, X. Wang, Efficient and long-time accurate second-order methods for Stokes-Darcy system, SIAM J. Numer. Anal. 51 (5) (2012) 493–497.
[15] W. Layton, H. Tran, C. Trenchea, Analysis of long time stability and errors of two partitioned methods for uncoupling evolutionary groundwater-surface water flows, SIAM J. Numer. Anal. 51 (1) (2013) 248–272.
[16] W. Chen, M. Gunzburger, D. Sun, X. Wang, An efficient and long-time accurate third-order algorithm for the Stokes-Darcy system, Numer. Math. 134 (4) (2016) 857–879.
[17] M.G. Armentano, M.L. Stockdale, Approximations by MINI mixed finite element for the Stokes-Darcy coupled problem on curved domains, Int. J. Numer. Anal. Model. 18 (2) (2021) 203–234.
[18] G. Du, L. Zuo, A two-grid method with backtracking for the mixed Stokes/Darcy model, J. Numer. Math. 29 (1) (2021) 39–46.
[19] S. Tlupova, A domain decomposition solution of the Stokes-Darcy system in 3D based on boundary integrals, J. Comput. Phys. 450 (2022).
[20] Yi Qin, Yang Wang, Yanren Hou, Jian Li, An unconditionally stable artificial compression method for the time-dependent groundwater-surface water flows, Numer. Methods Partial Differ. Equ. 39 (5) (2023) 3705–3724.
[21] M. Mu, X. Zhu, Decoupled schemes for a non-stationary mixed Stokes-Darcy model, Math. Comput. 79 (270) (2010) 707–731.
[22] L. Shan, H. Zheng, W.J. Layton, A decoupling method with different subdomain time steps for the nonstationary Stokes-Darcy models, Numer. Methods Partial Differ. Equ. 29 (2) (2013) 549–583.
[23] Y. Li, Y. Hou, A second-order partitioned method with different subdomain time steps for the evolutionary Stokes-Darcy system, Math. Methods Appl. Sci. 41 (5) (2018) 2178–2208.
[24] R. Li, J. Chen, Z. Chen, Y. Gao, A decoupled scheme with leap-frog multi-time step for non-stationary Stokes-Darcy system, Int. J. Comput. Math. (2017) 1–29.
[25] D. Xue, Y. Hou, A second-order decoupled algorithm with different subdomain time steps for the non-stationary Stokes/Darcy model, Numer. Algorithms 88 (2021) 1137–1182.
[26] P. Chidyagwai, A second order multirate scheme for the evolutionary Stokes–Darcy model, Appl. Numer. Math. 170 (2021) 364–383.
[27] N. Jiang, Y. Li, H. Yang, A second order ensemble method with different subdomain time steps for simulating coupled surface-groundwater flows, Numer. Methods Partial Differ. Equ. 38 (6) (2021) 1880–1970.
[28] Y. Qin, L. Chen, Y. Wang, Y. Li, J. Li, An adaptive time-stepping DLN decoupled algorithm for the coupled Stokes-Darcy model, Appl. Numer. Math. 188 (2023) 106–128.
[29] W. Chen, M. Gunzburger, F. Hua, X. Wang, A parallel Robin-Robin domain decomposition method for the Stokes-Darcy system, SIAM J. Numer. Anal. 49 (3) (2011) 1064–1084.
[30] Y. Cao, M. Gunzburger Xiaoming, X. He, X. Wang, Parallel, non-iterative, multi-physics domain decomposition methods for time-dependent Stokes-Darcy systems, Math. Comput. 83 (288) (2014) 1617–1644.
[31] G. Du, L. Zuo, Local and parallel finite element methods for the coupled Stokes/Darcy model, Numer. Algorithms 87 (4) (2021).
[32] J.L. Lions, Y. Maday, G. Turinici, A "parareal" in time discretization of PDE's, C. R. Acad. Sci., Ser. 1 Math. 332 (7) (2001) 661–668.
[33] Martin J. Gander, Stefan Vandewalle, Analysis of the parareal time-parallel time-integration method, SIAM J. Sci. Comput. 29 (2007) 556–578.
[34] G. Bal, On the convergence and the stability of the parareal algorithm to solve partial differential equations, in: The 15th International Domain Decomposition Conference, Springer Berlin Heidelberg, 2003, pp. 425–432.
[35] M.L. Minion, A hybrid parareal spectral deferred corrections method, Commun. Appl. Math. Comput. Sci. 5 (5) (2011) 265–301.
[36] Y. Maday, O. Mula, An adaptive parareal algorithm, J. Comput. Appl. Math. 377 (2020) 112915.
[37] S. Wu, T. Zhou, Fast parareal iterations for fractional diffusion equations, J. Comput. Phys. 329 (2017) 210–226.
[38] J. Dabaghi, Y. Maday, A. Zoia, A hybrid parareal Monte Carlo algorithm for parabolic problems, J. Comput. Appl. Math. 420 (2022) 114800.
[39] R.D. Falgout, T.A. Manteuffel, B. O'Neill, J. Schroder, Multigrid reduction in time for nonlinear parabolic problems: a case study, SIAM J. Sci. Comput. 39 (5) (2017) S298–S322.
[40] F. Legoll, T. Lelievre, U. Sharma, An adaptive parareal algorithm: application to the simulation of molecular dynamics trajectories, SIAM J. Sci. Comput. 44 (1) (2022) B146–B176.
[41] K. Pentland, M. Tamborrino, D. Samaddar, L.C. Appel, Stochastic parareal: an application of probabilistic methods to time-parallelization, SIAM J. Sci. Comput. 45 (3) (2023) S82–S102.
[42] D. Xue, Y. Hou, W. Liu, Analysis of the parareal method with spectral deferred correction method for the Stokes/Darcy equations, Appl. Math. Comput. 387 (2020) 124625.
[43] A. Dutt, L. Greengard, V. Rokhlin, Spectral deferred correction methods for ordinary differential equations, BIT Numer. Math. 40 (2) (2000) 241–266.
[44] M.L. Minion, Semi-implicit projection methods for incompressible flow based on spectral deferred corrections, Appl. Numer. Math. 48 (3) (2004) 369–387.
[45] S. Zhai, Z. Weng, Q. Zhuang, L. Fawang, V. Anh, An effective operator splitting method based on spectral deferred correction for the fractional Gray-Scott model, J. Comput. Appl. Math. 425 (2023) 114959.